International Journal of Nanomedicine

Dovepress
open access to scientific and medical research

Open Access Full Text Article

ORIGINAL RESEARCH

CD-340 functionalized doxorubicin-loaded nanoparticle induces apoptosis and reduces tumor volume along with drug-related cardiotoxicity in mice

This article was published in the following Dove Press journal:
International Journal of Nanomedicine

Laboni Mondal[1]
Biswajit Mukherjee[1]
Kaushik Das[2]
Sanchari Bhattacharya[1]
Debasmita Dutta[1]
Shreyasi Chakraborty[1]
Murari Mohan Pal[1]
Raghuvir H Gaonkar[3]
Mita Chatterjee Debnath[3]

[1]Department of Pharmaceutical Technology, Jadavpur University, Kolkata 700032, India; [2]Department of Biological Chemistry, Indian Association for the Cultivation of Science, Kolkata 700032, India; [3]Infectious Diseases and Immunology Division, CSIR-Indian Institute of Chemical Biology, Kolkata 700032, India

Background and objective: Targeted drug delivery of nanoparticles decorated with site-specific recognition ligands is of considerable interest to minimize cytotoxicity of chemotherapeutics in the normal cells. The study was designed to develop CD-340 antibody-conjugated polylactic-co-glycolic acid (PLGA) nanoparticles loaded with a highly water-soluble potent anticancer drug, doxorubicin (DOX), to specifically deliver entrapped DOX to breast cancer cells.

Methods: The study showed how to incorporate water-soluble drug in a hydrophobic PLGA (85:15) based matrix which otherwise shows poor drug loading due to leaching effect. The optimized formulation was covalently conjugated to anti-human epidermal growth factor receptor-2 (HER2) antibody (CD-340). Surface conjugation of the ligand was assessed by flow cytometry, confocal microscopy, and gel electrophoresis. Selectivity and cytotoxicity of the experimental nanoparticles were tested on human breast cancer cells SKBR-3, MCF-7, and MDA-MB-231. Both CD-340-conjugated and unconjugated nanoparticles were undergone in vitro and in vivo characterization.

Result: Higher level of incorporation of DOX (8.5% W/W), which otherwise shows poor drug loading due to leaching effect of the highly water-soluble drug, was seen in this method. In HER2-overexpressing tumor xenograft model, radiolabeled antibody-conjugated nanoparticles showed preferentially more of the formulation accumulation in the tumor area when compared to the treatments with the unconjugated one or with the other control groups of mice. The ligand conjugated nanoparticles showed considerable potential in reduction of tumor growth and cardiac toxicity of DOX in mice, a prominent side-effect of the drug.

Conclusion: In conclusion, CD-340-conjugated PLGA nanoparticles containing DOX preferentially delivered encapsulated drug to the breast cancer cells and in breast tumor and reduced the breast tumor cells by apoptosis. Site-specific delivery of the formulation to neoplastic cells did not affect normal cells and showed a drastic reduction of DOX-related cardiotoxicity.

Keywords: breast cancer, nanoparticles, ligand, targeting, tumor

Correspondence: Biswajit Mukherjee
Department of Pharmaceutical Technology, Jadavpur University, Kolkata 700032, India
Tel +91 332 457 2588
Fax +91 332 414 6677
Email biswajit.mukherjee@jadavpuruniversity.in

Introduction

Cancer is a major cause of death in the global population. In women, the most common malignant cancer is breast cancer which is the second major cause of cancer-related death in humans.[1] Non-specificity to deliver drug only to cancer cells and high level of cytotoxicity in normal cells become a major clinical challenge of

the present conventional breast cancer chemotherapeutics. Hence, it is important to specifically deliver therapeutic agent to the neoplastic cells without affecting the normal cells. Doxorubicin (DOX) is a commonly used anticancer drug in breast cancer which faces restriction in clinical use due to its dose-dependent toxicity such as cardiotoxicity and myelosuppression due to the non-selective nature of the chemotherapeutic agent.[2] Nanoparticulate carrier loaded with DOX may potentiate the transport of the incorporated drug to cancer cells by utilizing the tumor pathophysiology of enhanced permeability and retention (EPR) effects and tumor microenvironments.[3,4] Nanosized drug delivery system has shown their potential in cancer chemotherapy.[5] Biodegradable polymer poly(lactic-co-glycolic acid) (PLGA) based nanoparticle emerges as a promising drug carrier to treat many diseases including cancers.[2] The sustained drug release, biocompatibility, enhanced cellular internalization capability, increasing accumulation of the formulation in tumor by EPR effects, and enhanced stability of the formulation in blood are some of the added advantages of the PLGA-based drug nanocarriers. Various current efforts to deliver DOX in cancer cells have been reported in the literature.

A very recent approach for cancer treatment through mitochondria specific targeting has been evaluated by Xi et al 2018.[6] They studied the effect of functionalization the anticancer drug DOX with a hydrophobic tail conjugation by solubility promoting poly (ethylene) glycol polymer that resulted in prolonged circulation time and high tumor accumulation. Amphiphilic copolymer-based nanoparticulate drug delivery of DOX was demonstrated by Lv et al 2013.[7] Drug delivery to cancer cells via electrostatic interactions was a key factor for cancer treatment. Significant tumor accumulation of DOX through these amphiphilic nanoparticles was observed in xenograft mice model bearing non-small cell lung cancer. Gabizon et al, 2003 represented the pharmacokinetic profile of Pegylated liposomal DOX (doxorubicin liposome injection; Doxil® or Caelyx®)[8] characterized by longer blood circulation time and higher tumor uptake of doxorubicin.

Other efforts include ligand-mediated drug targeting. Biomarkers could be a good choice for the targeted delivery of therapeutic agent specifically to the breast cancer cells. The tumor progression is often associated with the overexpression of certain tumor antigen(s) on the surface of cancerous cells compared to the normal cells.[9] Current researchers have gained sufficient focus on targeting these surface proteins through complimentary antibody for more efficacies in cancer treatment.[10] Recent advances in nanotechnology have shown the way toward developing target-specific drug delivery system. Decoration of the surface of the delivery system with cell antigen-specific antibody can provide the enhanced target-specific delivery of encapsulated anticancer drug. This increased concentration of loaded drug in the target site through nanoparticulate system also reduces the systemic toxicity.[11] The ligand attached to the nanoparticles could help specifically delivering drug to the neoplastic cells.[12] Among many such ligands, monoclonal antibodies have also shown their potential to target-specific delivery of drug carriers.[13]

Human epidermal growth factor receptor-2 (HER2) is such a surface antigen that is overexpressed in breast cancer cells while the expression is limited in normal breast cell.[14] Normally, HER2 receptors help a healthy breast cell to grow, divide, and repair itself. In about 25% of the breast cancers, the HER2 gene malfunctions and make multiple copies of it commonly known as HER2 gene amplification. This leads to HER2 protein overexpression in breast cancer cell which makes breast cells grow and divide in an uncontrolled way.[15] CD-340 is also a type of HER2 protein which overexpresses more specifically by many breast cancer cells.[16]

The objective of this study was to design and develop doxorubicin-loaded PLGA nanoparticles conjugated with a specific ligand, HER2 antibody CD-340, to deliver the incorporated drug specifically to breast cancer cells, without much affecting normal cells to reduce drug-related cytotoxicity.

Materials and methods

Materials

Doxorubicin, (7S, 9S)-7-[(2R, 4S, 5S, 6S)-4-amino-5-hydroxy-6-methyloxan-2-yl]oxy-6,9,11-trihydroxy-9-(2-hydroxyacetyl)-4-methoxy-8,10-dihydro-7H-tetracene-5,12-dione), was a gift sample from Sun Pharmaceutical, Gujrat, India. PLGA {poly (lactide-co-glycolide) ratio 85:15, MW 50,000–75,000} was procured from Sigma-Aldrich Co, St Louis, MO, USA. Polyvinyl alcohol was purchased from SD Fine-Chemicals limited, Mumbai, India. Dimethylsulfoxide (DMSO) and dichloromethane (DCM) were procured from Merck Life Science Pvt. Ltd, Bengaluru, India. Pluronic F-68 was purchased from Himedia Laboratories Pvt. Ltd. Mumbai, India. Tween 80 was procured from SD Fine-Chemicals limited, Mumbai, India, D-α-Tocopherol polyethylene glycol

succinate (TPGS), Pluronic F127 and Suberic acid bis (3-sulfo-N-hydroxy succinimide ester) (BS3) were purchased from Sigma-Aldrich Co, St Louis, MO, USA. FITC anti-human CD-340 (erb B2/HER-2) was purchased from Biolegend, San Diego, California, United States. The media were procured from Himedia Laboratories Pvt. Ltd. Mumbai, India. 4',6' diamidino-2-phenylindole (DAPI) dye was procured from Thermo Fisher Scientific, Waltham, MA USA.

Cell culture and animals

Three different types of human breast cancer cells such as SKBR-3 cells (which overexpress HER2), MCF-7 (which weakly express HER2), and MDA-MB-231cells (which do not express HER2) were used. The cells were purchased from National Centre for Cell Science, Pune, India. Cell lines were maintained in McCoy's 5A media (for SKBR-3 cells)/ Dulbecco′s Modified Eagle′s medium (for MCF-7 and MDA-MB-231 cells). The media were supplemented with 10% fetal bovine serum (FBS, Sigma-Aldrich Co), 100 U/mL penicillin, 100 U/mL streptomycin and the cells were cultured in the respective medium in 5% CO_2 incubator (MCO-15AC; Sanyo, Tokyo, Japan) at 37°C.

Female BALB/c mice and athymic nude mice were procured from the National Institute of Nutrition (NIN), Hyderabad, India. All the animal studies were conducted upon receiving the approval of the Animal Ethics Committee (AEC), Jadavpur University, Kolkata and by following its guidelines.

Preparation of PLGA nanoparticles

A modified methodology has been adopted to incorporate the highly water-soluble DOX in PLGA nanoparticles. Adjustment of pH of the aqueous medium was significant to obtain higher loading of the drug in nanoparticles. Different formulations with different stabilizers were developed by following the multiple emulsion solvent evaporation method as described by Maji et al.[17] Blank nanoparticles (BL-NP) were formed without incorporating the drug in nanoparticles. All these formulation variations have been shown in Table 1. Detailed methodology has been described in the supplementary file.

Preparation of surface-functionalized PLGA nanoparticles (DOX-BS-NP)

Surface functionalization of PLGA nanoparticles was done by adding 0.5 mg/mL BS3[18] in the aqueous phase of 1.5%

Table 1 Composition of various experimental nanoparticle formulations with their physicochemical characteristics

Formulation	PLGA:Drug: DCM (Ratio by weight)	Sabilizer used	Average particle diameter (Z-average) (nm)	Polydispersity index[a]	Zeta potential (mV)	%Drug loading[a]	%Entrapment efficiency[a]
PVA	40:4:1	PVA (2.5% w/v)	357	0.398±0.03	−7.39±0.008	5±0.02	55%±0.3
PVA+TWEEN	40:4:1	PVA (2.5% w/v) &Tween 80 (14% v/v) (F2)	220	0.234±0.01	−14.7±0.009	8.5±0.015	93.5%±0.21
PVA+PLU-68	40:4:1	PVA (2.5% w/v) & Pluronic-68 (0.5% w/v)	449	0.041±0.018	−12.2±0.01	7±0.12	77%±0.5
PVA+PLU-127	40:4:1	PVA (2.5% w/v) & Pluronic-127 (0.5% w/v)	466	0.419±0.022	−13.7±0.011	6.9±0.03	75%±0.33
PVA+TPGS	40:4:1	PVA (2.5% w/v) & TPGS (0.03%w/v)	640	0.925±0.011	−9.98±0.008	6.03±0.15	66%±0.83
Antibody- conjugated formulation	40:4:1	PVA (2.5% w/v) &Tween 80 (14% v/v)	241	0.230±0.009	−2.93±0.013	8±0.01	88%±0.17

Note: [a]Each value represents mean ± SD (n=3).
Abbreviations: PLGA, poly (lactide-co-glycolide); DCM, dichloromethane; PVA, poly(vinyl alcohol); TWEEN, tween 80; PLU-68, pluronic F68; PLU-127, pluronic F127; TPGS, D -α-tocopherol polyethylene glycol succinate.

poly (vinyl alcohol) (PVA) solution. The remaining steps were the same as described above for nanoparticle formation.

Fourier transform infrared (FTIR) spectroscopy

Any interaction between the drug and excipients used in the formulation was investigated by FTIR spectroscopy.[18] For that purpose pure DOX, the excipients used, the physical mixture of DOX and the excipients, formulations with and without the drug (each on a separate basis) were investigated. All the samples were mixed with IR grade potassium bromide (1:100 ratio) and the pellet was formed by compressing in a hydraulic press. Scanning of the pellets was done over a wavenumber range of 4000–400 cm^{-1} in FTIR instrument (Magna-IR 750, Series II, Nicolet Instruments Inc, Madison, Wisconsin, USA). FTIR analysis was performed for BS3 and BS3-functionalized nanoparticles to confirm that BS3 indeed inserted on the surface of nanoparticles. Pellet formation and analysis procedure were the same as mentioned earlier.

Characterization of DOX-NP

Detail of the following methodologies for characterization has been described in supplementary file.

Determination of drug loading

DOX-NP (2 mg) was dissolved in DMSO (2 mL), sonicated (for 30 mins), and centrifuged (16,000 rpm, for 10 mins). Absorbance of the supernatant was read against blank at 480 nm in the UV-Visible (UV-VIS) spectrophotometer (Intech-295, Intech corporation, Warsaw, Poland). The percentage of drug loading and drug loading efficiency were calculated using the respective equations described earlier.[17,19]

Particle size and zeta potential

Lyophilized DOX-NP and DOX-Ab-NP were resuspended in Milli-Q water (2 mL), sonicated (for 15 mins), vortexed (for few mins,) and subjected to analysis for average particle size, polydispersity indices (PDI) and zeta potential using the Zetasizer Nano ZS 90 (Malvern Instruments, Malvern, UK) instrument as described by Dutta et al.[20]

Morphological characteristics of nanoparticles

Morphology of the developed nanoparticles was analyzed by scanning electron microscope (SEM), transmission electron microscopy (TEM), atomic force microscopy (AFM) as methods described by Bhattacharya et al.[21]

In-vitro drug release & drug release kinetic study

The freeze-dried DOX-NP (2 mg) was weighed accurately and resuspended in phosphate-buffered saline (PBS) (pH 7.4) and incubated at 37°C in an incubator shaker (BOD-INC-1S, Incon, India) with light agitation (60 rpm). Individual samples (1 mL) were collected at a predetermined time interval after centrifugation (in a cold centrifuge, at 16,000 rpm for 10 mins) (Hermile Labortechnik GmbH, Wehingen, Germany) and the volume withdrawn was replaced with 1 mL fresh PBS (pH 7.4). Pellets at the bottom were resuspended by vortexing and samples were again kept in incubator shaker till next sampling. The amount of the drug present in the collected samples was determined by UV-VIS spectrophotometer at 480 nm against fresh PBS (pH 7.4) as blank. Similar procedure was followed to determine the pattern of release of drug from the optimized formulation in different buffers (having different pH, such as citrate buffer (pH 3), acetate buffer (pH 5), and bicarbonate buffer (pH 10) and different media (PBS release media added with hydroxypropyl β –cyclodextrin (HBC)/tween 80) mimicking in vivo drug release media, i.e., blood.[20]

Antibody conjugation on the nanoparticle surface

A weighed amount of lyophilized surface-functionalized (with BS3) nanoparticles (DOX-BS-NP) (1 mg) was resuspended in PBS (1 mL). 1 µL anti-HER2 antibody (from the stock of 400 ng/mL) was added to that 1 mL of the sample solution. After brief vortexing, the samples were incubated at room temperature (25°C) for 1 hr that was followed by centrifugation (at 16,000 rpm for 10 mins) to remove unattached antibodies. The pellet was collected and resuspended and further washed three times to remove any unconjugated (free) antibody on the nanoparticle surface. After lyophilization, the product was stored at 4°C until further use.[22]

Determination of antibody conjugation on the surface of PLGA nanoparticles

The following methods were used to confirm conjugation of anti-HER2 antibody on the DOX-NP surface.

Flow cytometry

A dispersion of DOX-NP conjugated with FITC-labeled anti-HER2 antibody ligand was analyzed by FAC Scan flow cytometer (Becton Dickinson, San Jose, CA)

(FACS) and unconjugated NPs were analyzed simultaneously as a control.[23,24]

Laser-scanning confocal microscopy

FITC-labeled anti-HER2 antibody-conjugated blank NPs (nanoparticles without drug) were redispersed in PBS (pH 7.4). One drop of the sample was cast on a clean glass slide and a coverslip was fixed on it using dibutyl phthalate polystyrene xylene. Localization of FITC (tagged only with antibody) was observed under Confocal Spectral Microscope (TCS-SP8 confocal microscope, Leica, Germany).[23]

SDS-PAGE gel electrophoresis

SDS-PAGE gel electrophoresis study was performed to determine the conjugation of antibodies on the surface of DOX-NP. Briefly, DOX-NP and DOX-Ab-NP were resuspended in PBS buffer (20 µL from 10 mg/mL stock) and free antibody (1 µL) was mixed separately with 2X Laemmli gel loading buffer (5 µL each). The samples were loaded to a 10% SDS-PAGE gel along with the marker. The gel was run for 80 V up to stacking and 100 V up to resolving. After gel electrophoresis, the protein was transferred onto polyvenylidene difluoride (PVDF) membrane (run time 1 hr with 15 V) and incubated with primary antibody. Membranes were blocked with 5% bovine serum albumin (BSA) in Tris buffer saline (TBS) and incubated overnight at 4°C with secondary antibodies against HER2 (1:5000; Cell Signaling Technology, CST or Abcam). After four times washing (10 min interval) with TBS-tween 20 (0.1%), development was done by Enhanced Chemi-Luminescent (ECL) method.[25]

Characterization of DOX-Ab-NP with SEM, AFM, and TEM

For analysis of antibody-conjugated nanoparticles by SEM, AFM, and TEM, the same procedure was followed as mentioned earlier for DOX-NP.

Stability study

Accelerated stability analysis

A stability study was performed to understand the effect of temperature and relative humidity on DOX-NP, and DOX-Ab-NP storing them at 4–8°C (in refrigerator), 30°C, 75% RH, and 40°C, 75% RH for 30, 60, and 90 days as per the International Conference on Harmonization (ICH) guidelines (ICH, 2003). Detailed methodology has been given in the supplementary file.

Hydrolytic stability study

The formulations were further analyzed for hydrolytic stability at different pH buffers (citrate buffer pH 3, acetate buffer pH 5, phosphate buffer pH 7.4, and bicarbonate buffer pH 10) for 30 days as described by Mandal et al.[26] Detailed methodology has been given in the supplementary file.

In-vitro cellular studies

Assessment of cytotoxicity by MTT assay

Cytotoxicity of DOX, DOX-NP, and DOX-Ab-NP were determined in time-dependent manner on three different breast cancer-specific cell lines (i.e. SKBR-3, MCF-7, and MDA-MB-231) that differ in their expression level of HER2 antigen on their surface. MTT (3-(4, 5-dimethylthiazol-2-yl)-2, 5-diphenyl tetrazolium bromide)[27] assay was performed as per the reported method by Zeng et al.[28] The antiproliferative effect of DOX, DOX-NP, and DOX-Ab-NP was calculated as a percentage of cell growth inhibition with respect to dose and compared to the respective controls. Detailed methodology has been given in the supplementary file.

Cellular internalization of nanoparticles by confocal microscopy

Binding and internalization of DOX-NP and DOX-Ab-NP in HER2-overexpressing cells and HER2 negative cells were examined by confocal microscope (TCS-SP8 confocal microscope, Leica, Germany) as described by Chen et al.[23] Detailed methodology has been given in the supplementary file.

Apoptosis study by annexin v FITC

SKBR-3 cells were seeded into six-well culture plates with Macoy's media at 37°C at a concentration of 1×10^5 cells per well. The apoptosis of cells exposed to DOX (at its IC_{50}), DOX-NP, and DOX-Ab-NP (at their respective IC_{50} values) for 24 hrs were determined. After 24 hrs incubation, the cells were trypsinized, pelleted with centrifugation (at 3000 rpm for 3 mins), washed with PBS and finally stained with FITC-labeled Annexin V and propidium iodide and apoptosis was quantified using flow cytometry.[29]

Cell cycle distribution analysis

The effects of DOX-NP and DOX-Ab-NP on cell cycle progression and population were studied by FACS. SKBR-3 cells were seeded in a six-well plate at 1×10^5 cells per well. The cells were treated with the respective

IC_{50} values of DOX, DOX-NP, and DOX-Ab-NP. After 24 hrs incubation period, cells were collected, washed (thrice with sterile PBS, pH 7.4) to remove uninternalized drug or nanoparticles. After cell fixation with chilled ethanol (70%), the cells were treated with propidium iodide (20 µg/mL) for 30 mins. DNA content was measured for 15,000 events for each sample (FACS VerseTM machine (BD biosciences, San Jose, USA). Cell cycle arrest was detected by comparing the data with the control sample.[27]

Caspase activation

Determination of the relative level of HER2 antigen in breast cancer cells

The relative levels of HER2 in SKBR-3, MCF-7, and MDA-MB-231 cells were analyzed in a comparative approach as described by Ding et al.[30] The cells were lysed with Laemmli buffer and the protein lysate was loaded onto SDS-PAGE gels. The protein was transferred onto the PVDF membrane (run time 1 hr with 15 V). After blocking the membrane with 5% BSA in TBS, incubation with primary antibody was done overnight against HER2 (1:5000) followed by incubation with HRP-tagged secondary antibody (1:5000; anti-mouse; Sigma) and then subjected to development by the ECL method. The stripped membrane was used for determination of the respective β-actin proteins. Band intensity was measured by Image J. Detailed methodology has been provided in the supplementary file.

Caspase 3/7 activity assay

Caspase 3/7 activity was measured in SKBR-3, MCF-7, and MDA-MB-231 cells after challenging the cells with DOX/DOX-NP/DOX-Ab-NP (at their respective IC_{50} values) for 24 hrs in a fluorimetric approach using caspase 3/7 assay kit (Abcam; ab39401) as per the method described by Peterson et al.[31] The comparative graphical analysis was performed by GraphPad Prism 5. Detailed methodology was described in the supplementary file.

Detection of PARP cleavage

SKBR-3, MCF-7, and MDA-MB-231 cells were seeded onto 24-well plates and exposed to DOX/DOX-NP/DOX-Ab-NP (at their repective IC_{50} values). After 24 hrs of treatment, media were removed; cells were lysed with 2X Laemmli Buffer and the lysate was subjected to analysis of PARP cleavage by Western blotting with PARP1 specific antibody (CST). Densitometric scanning of the blots was performed by Image J and accordingly, quantification was made.

In vivo studies

Pharmacokinetic study

Pharmacokinetic and biodistribution parameters were analyzed in BALB/c mice using free DOX (10 mg/kg), DOX-NP, and DOX-Ab-NP (containing an equivalent amount of free DOX). Animals (bodyweight 25–30 g) were divided into four groups (n=3). The first group was the untreated control group. In the second, third, and fourth groups, the mice were treated with IV administration of free-DOX, DOX-NP, and DOX-Ab-NP, respectively. The treated animals were sacrificed in predetermined time points (at 0.5, 1, 2, 4, 6, 8, 10, 12, 24, 48, and 96 hrs, after injection). Blood was collected by a cardiac puncture; plasma was separated. LC-MS/MS was performed to quantify drug by protein precipitation technique.[32]

Detailed methodology has been described in the supplementary file.

Cardiac toxicity study

Doxorubicin-induced cardiotoxicity was studied in 15 female BALB/c mice (~25 g each) (group=5, normal control, and 4 treated groups, n=3). Group I mice were kept as the control (animals without any treatment), Group II animals were treated with IV blank (without drug) nanoparticles, Group III animals were treated with IV administration of free-DOX, Group IV and Group V animals were treated with DOX-NP and DOX-Ab-NP, respectively (amount of NP administered had drug equivalent to free DOX). In the treatment groups, the animals were treated with DOX/DOX-NP/DOX-Ab-NP in three consecutive injections with a total amount of 18 mg DOX.[33,34] Mice in the control group received saline each time. The bodyweight of the animals was recorded after every 48 hrs during the study period. After 14 days of injection (i.e., last dose), the animals were lightly anesthetized for the measurement of the electrocardiogram of the animals of different groups.

Mice were then sacrificed, blood was collected, and serum was separated. Creatine phosphokinase (CK-MB), and lactate dehydrogenase (LDH) enzyme activities were measured in the serum and superoxide dismutase (SOD) level was determined in the heart homogenate (heart tissues were separated and homogenized in ice-cold PBS (10 mL/g tissue) using tissue homogenizer (Bio-Lab instruments, Mumbai, India)) using respective commercial kit according to manufacturer protocol (CK-MB (NAC act.) Kit, Tulip Diagnostics, India and Reckon Diagnostics P. Ltd, India)).

The weight of the isolated heart from each group of the mice was measured. A histopathological investigation was done after hematoxylin and eosin staining.[35]

In vivo breast tumor model

Animal model

All athymic nude mice (CAnN.Cg-Foxn, 6 weeks old, ~20 g) were obtained from NIN, Hyderabad, India. The solid tumor was induced in each mouse by inoculating SKBR-3 cells (1×10^7 in 200 µL medium) subcutaneously into the left rear flank of mice. The animals were maintained with their normal diet and water until the injected cells formed a solid tumor. In vivo experiments with those xenograft mice were performed when the size of the tumor had grown to approximately 100–150 mm^3.[36]

Radiolabelling of DOX, DOX-NP, and DOX-Ab-NP

Free-DOX (5 mg) was dissolved in ethanol (0.5 mL) and DOX nanoparticle formulations containing an equivalent amount of DOX were suspended in nitrogen-purged water. With the dispersion of drug/nanoparticles, the aqueous solution of ^{99m}Tc-pertechnetate ($^{99m}TcO^{4-}$) 185–300 MBq (200 µL) was added followed by addition of freshly prepared stannous chloride dehydrate solution (20 mg in 10 mL nitrogen-purged water containing 100 µL of 6 N HCl). These mixtures were at room temperature for 10−15 mins and stored in sealed vials for further use. The extent of radiolabelling was checked by Instant thin-layer chromatography using acetone and silica gel-coated aluminum sheets (Merck, Darmstadt, Germany) as mobile phase and as stationary phase, respectively. After the run, the sheet was dried and five strips of 1 cm each were cut for quantitative counting that was recorded in a well-type gamma counter (Electronic Corporation of India, model LV4755, Hyderabad, India) at 140 keV.

Gamma scintigraphy and biodistribution study

^{99m}Tc labeled DOX (^{99m}Tc-DOX)/^{99m}Tc labeled DOX-NP (^{99m}Tc-DOX-NP)/^{99m}Tc labeled DOX-Ab-NP (^{99m}Tc-DOX-Ab-NP)[37] were injected through tail vein in mice bearing solid breast tumor (Three groups of mice, each group contained three animals). Images were captured at 0.5 and 4 hrs post-injection, using a gamma camera (GE Infnia Gamma Camera equipped with Xeleris Work station, GE, Cleveland, OH, USA).

At the time point of 6 hrs after injection of ^{99m}Tc-DOX, ^{99m}Tc-DOX-NP, and ^{99m}Tc-DOX-Ab-NP, various organs and tissues including the solid tumors from respective tumor-bearing mice were excised, washed properly using normal saline, excess water was removed and then weighed. Blood samples were collected before tissue excision by cardiac puncture technique. From all the sample, radioactivity was measured using a well-type gamma scintillation counter along with an injection standard. The results were expressed as percent-injected dose per g of tissue or organ for biodistribution.[38]

In vivo therapeutic study on tumor-bearing xenograft mice

Therapeutic potency of the experimental DOX, DOX-NP, and DOX-Ab-NP was studied in mice bearing SKBR-3 tumor (Four tumor-bearing mouse groups; each group contained three animals). DOX/DOX-NP/DOX-Ab-NP/saline was injected IV to tumor bearing mice according to the requirement of the group, with three subsequent doses of DOX (3 mg/kg) on every alternate day in each case and the tumor volume was evaluated. Tumor sizes at definite time point were measured by slide caliper. At the same time, the body weights of the treated mice were monitored regularly to assess treatment-related toxicity.[36] After the sacrifice, the tumors were removed, weighed and were compared among the experimental groups of mice as referred above.

Statistical analysis

The data are presented as mean ± SD and were statistically analyzed by one-way ANOVA followed by Tukey's multiple comparisons, and statistical significance was considered at $p<0.05$.

Results

Physicochemical characterization of DOX-NP

FTIR

Doxorubicin possesses different reactive functional groups such as free NH_2, OH, and CO groups in its structure. Figure S1 depicted the FTIR spectra of DOX, the excipients, their physical mixture, and formulations. The band between wavenumbers 3400–3500 cm^{-1} is for N–H stretching and the band between wavenumbers 1550–1650 cm^{-1} is the range for N–H bending (1° amine) with medium stretching intensity. The wavenumber ranges between 1720 and 1740 cm^{-1} and 1710–1720 cm^{-1} are an indication for CO (saturated aldehyde) and C=O (saturated ketone) groups. In the FTIR spectra of DOX, the peak observed at 3524.56 cm^{-1} for primary amines, at 1615.85 cm^{-1} for N–H bending (1° amine), also at 1729.84 cm^{-1-} for CO group. In the

spectrum of PLGA, the peaks observed in the wavenumber range 2850–3000 cm^{-1} are for C–H stretching vibration of the alkyl groups. For the OH group of PLGA, the peak observed at 3494.5 cm^{-1} belongs to the range between wavenumbers 3200–3550 cm^{-1} for OH stretching. The typical ester C=O stretching band of PLGA was observed at 1756 cm^{-1}. In the FTIR spectrum of PVA, the observed broad peak at 3424.35 cm^{-1} is attributed to O–H stretching vibration. The peak observed at 1735.20 cm^{-1} is for C=O in (carbonyl) stretching band and the peak at 2926.79 cm^{-1} revealed the peak for C–H stretching vibration.

The peaks in FTIR spectra at 2400 and 2360 cm^{-1} (Figure S1) observed in DOX-BS-NP were responsible for BS3.[18]

In brief, the FTIR study revealed that no chemical reaction occurred between DOX and the excipients used in this study. While the minor shifting of peaks was only due to the physical interactions that provided for the formulation structure.

Drug loading and drug loading efficiency

Different surfactants such as tween 80, TPGS, pluronic-68, and pluronic-127 were used along with PVA to improve the drug loading (Table 1). Percentage loading was increased when co-surfactants were added with PVA in the formulations.

Particle size, zeta potential, and PDI

SEM images (Figure S2) showed that particle size distribution varied with the surfactants used. With PVA only, particle size was observed at 357 nm. The formulations made up of other surfactants such as pluronic F-68 and pluronic F-127 and TPGS (Figure S2G, J, and M, respectively) showed much larger particles when added along with PVA (449, 466, and 640 nm, respectively). However, tween 80 and PVA combination (Figure S2D) produced a smaller particle size of 220 nm which was considered for further studies. Nanoparticles with different surfactants showed negative zeta potentials (−7.39 ±0.008 mV, −14.7±0.009 mV, −12.2±0.01 mV, −13.7±0.011 mV, −9.98±0.008 mV) and PDI values were 0.398±0.03, 0.234±0.01, 0.041±0.018, 0.419±0.022, 0.925±0.011 for PVA, PVA with tween 80, PVA with pluronic F-68, PVA with pluronic F-127, and PVA with TPGS, respectively (Table 1). SEM images showed the better formation of particles with tween 80, with smooth surface and round in shape where formulations with other surfactants resulted in uneven surface formation of the particles (Figure S2F). From the data of drug loading, particle size, and SEM images, Formulation (PVA+TWEEN) (F2) was considered for further studies.

In the SEM images of DOX-Ab-NP, the surface was not smooth (Figure S2R) in comparison to the unconjugated nanoparticles. Particle size and zeta potential were found to increase for DOX-Ab-NP (Figure S2P and 2Q).

Atomic force microscopy (AFM)

AFM data (Figure 1A and B) showed that very small particles have conglomerated to form a nano-size cluster with a maximum height of 32.5 nm and amplitude value 19.5 mV and numbers of particles were forming a cluster. AFM images of DOX-Ab-NP showed rough surface properties due to the presence of the antibody on the surface (Figure 1B).

Transmission electron microscopy (TEM)

Internal morphology was verified with TEM analysis of the prepared nanoparticles. The images showed that the drug was well distributed throughout the particles in tiny particulate forms (Figure 1C and D). Further, the particles had no hollow structure inside and they were more or less solid in structure. TEM images (Figure 1D) indicated the presence of a FITC-conjugated antibody on the surface of the nanoparticles by an intense brighter shadow around the particle possibly due to the presence of FITC and it was absent for DOX-NP.

Energy dispersive x-ray (EDX) study

EDX analysis for weight % and atomic % of various elements (Table 2) of BL-NP, DOX-NP, BL-NP-BS, and DOX-BS-NP showed the presence of sulfur % only in BL-NP-BS and DOX-BS-NP, indicating the presence of BS3 as sulfur is one of its constituents.

In-vitro drug release and kinetic study

Fast drug release (97% in 6 hrs) in citrate buffer (pH 3) (Figure 2) suggested that polymers of the formulation (F2) degraded in acidic pH, hence would not be suitable for oral application. On the other hand, a very slow and steady release (27% in 5 months) of the drug in PBS (pH 7.4) indicates that this formulation would be stable in the blood (as pH 7.4 mimics the environment of blood) in vitro, for a long duration and would slowly degrade. In acetate buffer (pH 5.5), the formulation moderately released drug (65% in 5 months) which suggests that the nanoparticles would be stable in blood and upon distributions deliver the drug better in the tumor area which generally had an acidic environment (pH around 4.5–5.5).[36] In our previous work, we have shown the stability of drug-loaded PLGA nanoparticles in mouse serum at least for 24 hrs.[39] Further Chung et al 2010 showed that the surface-functionalized PLGA nanoparticles were stable when incubated in full

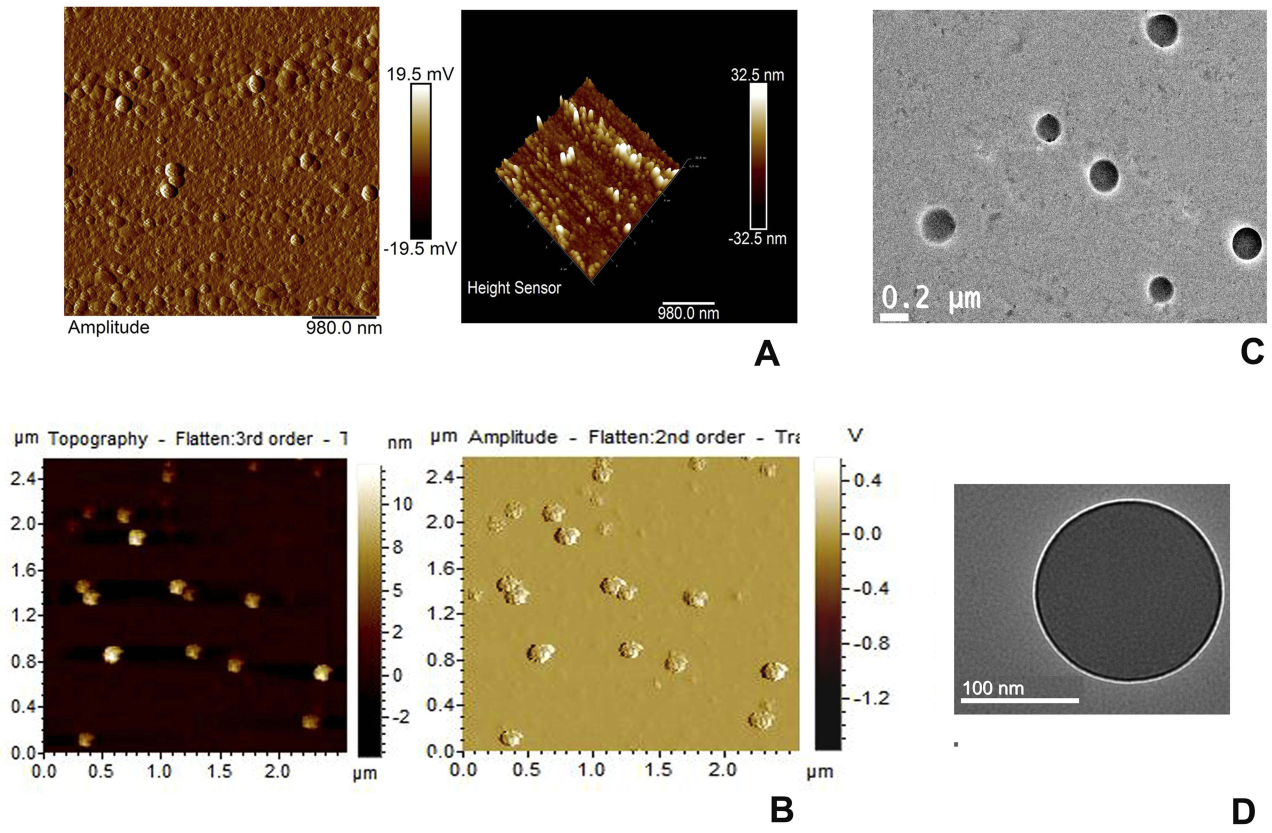

Figure 1 AFM and TEM images of experimental nanoparticles.
Notes: AFM (**A**) DOX-NP, (**B**) DOX-Ab-NP and TEM (**C**) DOX-NP and (**D**) DOX-Ab-NP.
Abbreviations: PLGA, polylactic-co-glycolic acid; PVA, poly (vinyl alcohol); AFM, Atomic force microscopy; DOX, doxorubicin; Ab, antibody; NP, nanoparticle; TEM, transmission electron microscopy.

serum condition (100% FBS) for overnight.[40] All these experimental results depicted the stability of PLGA nanoparticles in blood for prolonged period irrespective of their incorporated drugs.[7]

Release data were assessed using zero-order, first-order, Hixon–Crowell, Korsmeyer-Peppas, and Higuchi kinetic models represented in Table 3. Various regression coefficient (R^2) values for the kinetics were tabulated (Table 3). R^2 values suggest that drug release followed Higuchi kinetics in PBS (pH 7.4)/PBS with HβCD and bicarbonate buffer. In acetate buffer, citrate buffer, and PBS with tween 80 it followed Korsmeyer–Peppas kinetic model.

Table 2 Weight % and atomic % of elements in various nanoparticles

Sample	CK		OK		NK		NaK		SK	
	Weight %	Atomic %	Weight %	Atomic %	Weight %	Atomic %	Weight %	Atomic %	Weight %	Atomic %
BL-NP	42.13	49.64	56.86	50.29	-	-	-	-	-	-
DOX-NP	35.64	41.98	50.38	44.55	13.28	13.42	-	-	-	-
BL-NP -BS	40.84	48.63	34.28	30.65	18.48	18.87	2.47	1.54	0.07	0.03
DOX- BS-NP	34.29	42.41	48.84	45.35	10.37	11.00	1.24	0.80	0.08	0.04

Note: Weight % and atomic % of elements in various nanoparticles.
Abbreviations: CK, carbon counts; OK, oxygen counts; NK, nitrogen counts; NaK, sodium count; SK, sufur count; BL-NP, blank nanoparticles; DOX-NP, doxorubicin loaded PLGA nanoparticles; BL-NP-BS, blank nanoparticles cross-linked with BS3; DOX-BS-NP, doxorubicin-loaded PLGA nanoparticles cross-linked with BS3.

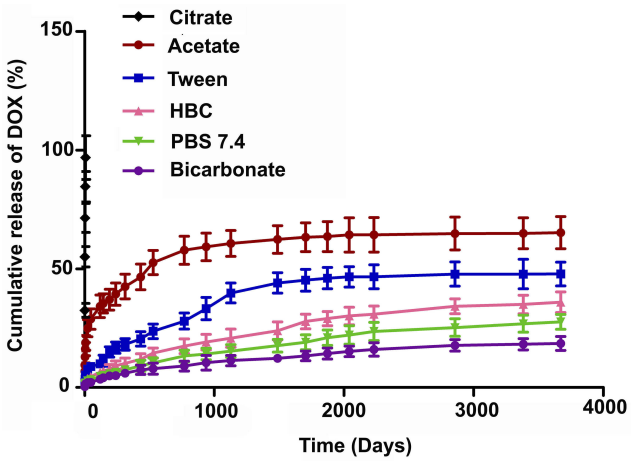

Figure 2 In-vitro drug release profile of DOX from DOX-NP in different buffers (citrate buffer (pH 3), acetate buffer (pH 5), phosphate buffer (pH 7.4), and bicarbonate buffer (pH 10)) and different media (PBS release media added with hydroxy propyl β-cyclodextrin (HBC)/TWEEN, tween 80). Data show mean±SD (n=3).

Abbreviations: PVA, poly (vinyl alcohol); TPGS, tocopherol polyethylene glycol succinate; DOX, doxorubicin; Ab, antibody; NP, nanoparticle.

Determination of antibody conjugation on nanoparticles

Flow cytometry

FACS analysis of FITC-labeled DOX-Ab-NP and DOX-NP showed the presence of fluorescence in DOX-Ab-NP only (Figure 3A and B), suggesting the successful attachment of the antibody to DOX-Ab-NP.

Laser-scanning confocal microscopy

Confocal microscopy showed FITC-labeled antibody was successfully conjugated on nanoparticles (Figure 3C). The figure shows that there were few scattered antibody-conjugated particles on the slide after dropping and drying a highly diluted suspension of the particles.

SDS-PAGE gel electrophoresis

In the gel electrophoresis (Figure 3D), the band for antibody-conjugated nanoparticles was found in the well, as the heavier nanoparticles could not move from the well. But free antibody moved according to its size.

Stability study

In a stability chamber

DOX-NP/DOX-Ab-NP stored at 4–8°C was found to maintain morphology (Figure S3C), and drug content throughout the period. The formulations stored at 30°C and 40°C also maintained their drug content and physicochemical stability but deformed morphologically during storage (Figure S3A and B).

Table 3 In-vitro drug release kinetic data tested on various release kinetic models with corresponding R^2 values and release exponent (n) (Korsmeyer–Peppas model)

	Phosphate- buffered saline pH 7.4	HBC	Tween	Acetate buffer pH 5	Citrate buffer pH 3	Bicarbonate buffer pH 10
Zero order	y=0.0077x +4.0662 R^2=0.9329	y=0.0102x +5.7819 R^2=0.92	y=0.0141x +11.237 R^2=0.8128	y=0.0141x +30.183 R^2=0.6313	y=10.308x +40.221 R^2=0.8679	y=0.0052x +3.1674 R^2=0.9068
First order	y=−4E-05x +1.9826 R^2=0.9504	y=−6E-05x +1.9751 R^2=0.9436	y=−9E-05x +1.9475 R^2=0.8463	y=−0.0001x +1.8338 R^2=0.7145	y=−0.2231x +1.929 R^2=0.9682	y=−2E-05x +1.9862 R^2=0.9209
Higuchi	y=0.464x +0.1319 R^2=0.9948	y=0.6156x +0.5097 R^2=0.9915	y=0.8914x +2.9913 R^2=0.9565	y=0.9629x +20.23 R^2=0.8611	y=34.366x +16.017 R^2=0.9446	y=0.3156x +0.4174 R^2=0.9958
Hixon–Crowell	y=−0.0001x +4.5791 R^2=0.9449	y=−0.0002x +4.5525 R^2=0.9362	y=−0.0003x +4.4589 R^2=0.8358	y=−0.0003x +4.0965 R^2=0.688	y=−0.4348x +4.104 R^2=0.9765	y=−9E-05x +4.5924 R^2=0.9163
Korsmeyer–Peppas	y=0.406x− 0.0626 R^2=0.9735 n=0.4	y=0.3856x +0.1296 R^2=0.9634 n=0.38	y=0.385x +0.3448 R^2=0.9776 n=0.38	y=0.2291x +1.0555 R^2=0.9833 n=0.22	y=0.3072x +1.7477 R^2=0.9921 n=0.3	y=0.4304x− 0.2729 R^2=0.9841 n=0.43

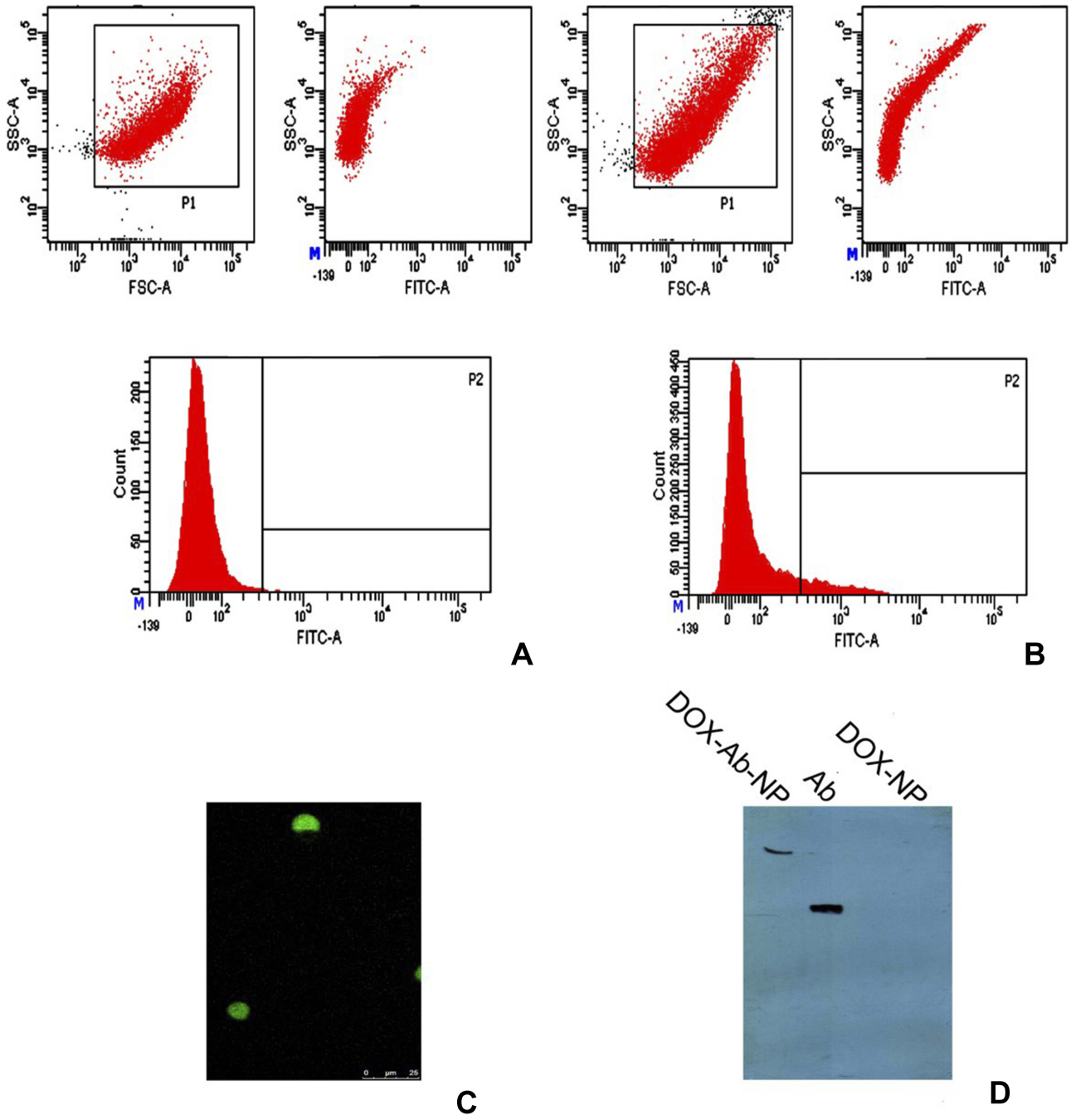

Figure 3 Different studies for confirmation of antibody conjugation on the surface of polylactic-co-glycolic acid (PLGA) nanoparticles.
Notes: (**A**) Flow cytometry data for unconjugated nanoparticles, (**B**) for antibody-conjugated nanoparticles, (**C**) laser-scanning confocal microscopy, showing FITC labeled CD-340 antibody-conjugated scattered nanoparticles and (**D**) SDS-PAGE gel electrophoresis, showing CD-340 antibody-conjugated NP, antibody unconjugated NP and free-antibody.
Abbreviations: DOX, doxorubicin; Ab, antibody; NP, nanoparticle.

Hydrolytic stability study

Weight loss of particles at the different time points showed that after 4 weeks, the mass loss of DOX at pH 3, pH 5, pH 7.4, and pH 10 was 93.17±0.73%, 45.45±1.32%, 38.47±0.98%, and 29.01±1.97%, respectively (Figure S3D). The higher hydrolytic stability of the nanoparticles was seen at higher pH values.

In-vitro cellular studies

Assessment of cytotoxicity by MTT assay

In MDA-MB-231 cells, IC_{50} value for free-DOX was 6.2 μM, that for DOX-NP was 4 μM and the value for DOX-Ab-NP was 3.8 μM. In the case of MCF-7 cells, IC_{50} value for free-DOX was 0.65 μM, for DOX-NP, the value

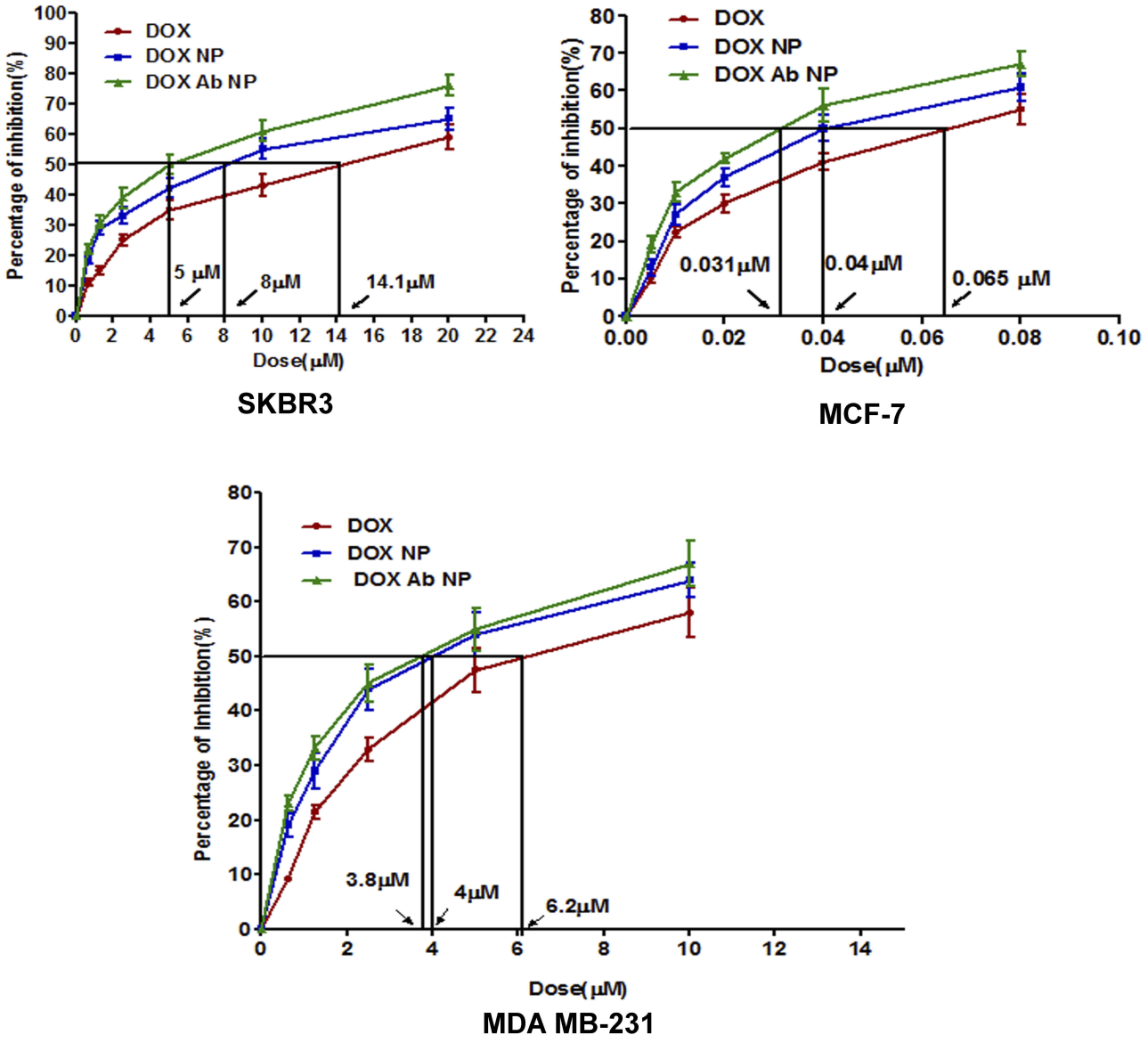

Figure 4 In-vitro cytotoxicity data of DOX, DOX-NP, and DOX-Ab-NP determined in SKBR-3 cells, MCF-7 cells, and MDA-MB-231 cells. Data show mean ±SD (n=3).
Abbreviations: DOX, doxorubicin; Ab, antibody; NP, nanoparticle.

was 0.4 μM and for DOX-Ab-NP, it was 0.31 μM. Again, for SKBR-3 cells the value of IC_{50} for DOX was 14.1 μM, for DOX-NP was 8 μM and for DOX-Ab-NP, the value was 5 μM (Figure 4). Thus, DOX-Ab-NP showed remarkably higher cytotoxicity in comparison to DOX-NP for HER2-mediated higher uptake by HER2-expressing cells.

Cellular internalization of nanoparticles by confocal microscopy

Confocal microscopic images (Figure 5) showed significantly higher–intracellular intensities for DOX-Ab-NP (red fluorescence due to DOX) than DOX-NP (red fluorescence due to DOX) in SKBR-3 cells than the other two types breast cancer cells which suggest the specific targeting capability of HER2 antibody in HER2 positive SKBR-3 cells. DAPI stained cells showed no fluorescence due to FITC in the case of MDA-MB-231 cells, moderate-intensity in MCF-7 cells and an intense fluorescence in SKBR-3 cells when treated with FITC labeled CD-340 antibody-conjugated BL-NP due to the presence of HER2 surface antigens.

Apoptosis study by annexin v FITC

Higher apoptotic level in FACS histogram (extent of apoptosis 19.6% for DOX, 33.6% for DOX-NP and 43.1% for DOX-Ab-NP) in SKBR3 cells treated with DOX-Ab-NP than the cells

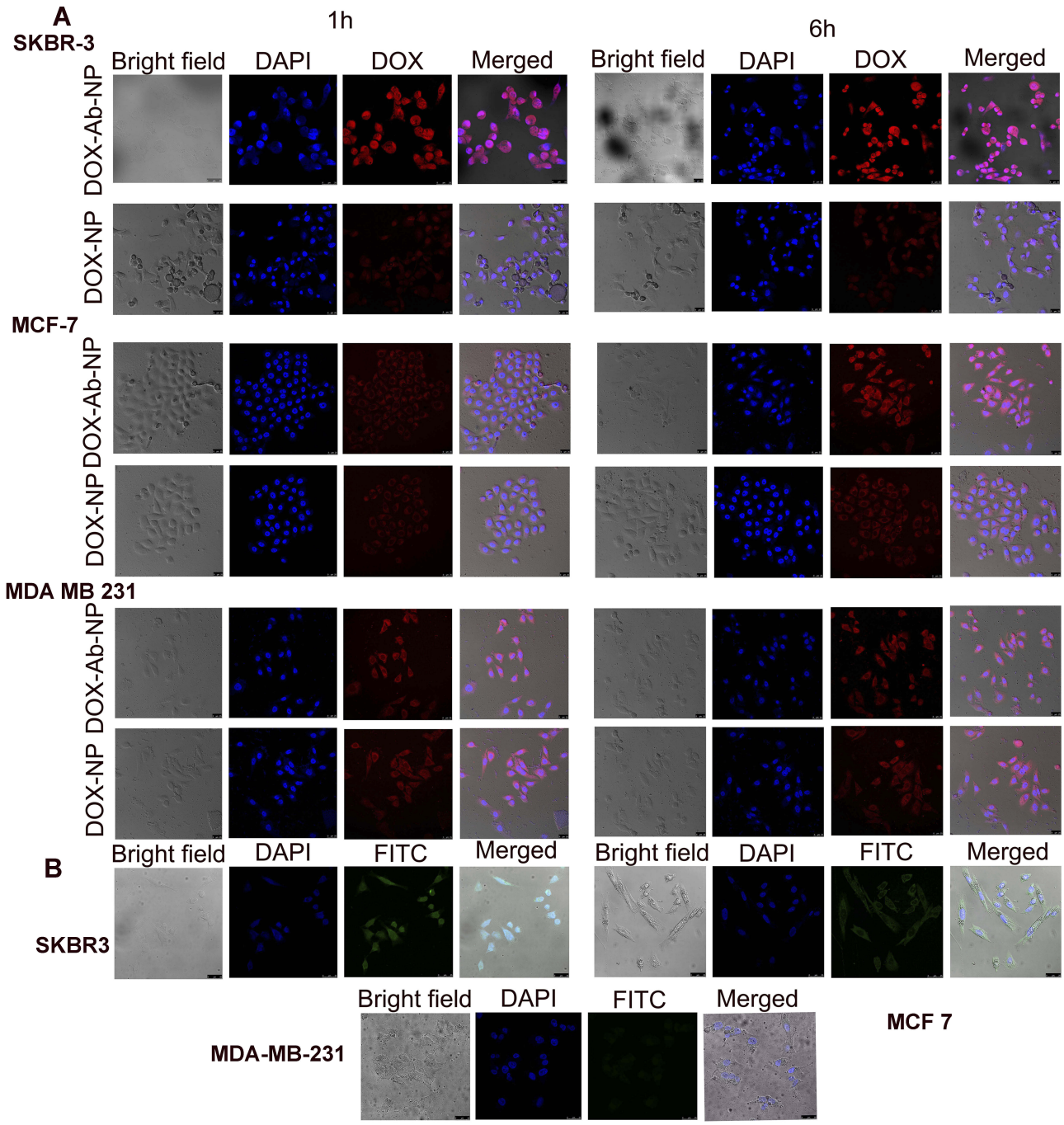

Figure 5 Cellular uptake of antibody conjugated and unconjugated nanoparticles in various cell lines.
Notes: (**A**) Cellular uptake of DOX-NP and DOX-Ab-NP in SKBR-3, MCF-7, and MDA-MB-231 cells observed by confocal microscopy at 1 and 6 hrs, respectively (**B**) Cellular uptake of antibody-conjugated blank nanoparticles in SKBR-3, MCF-7, and MDA-MB-231 cells observed by confocal microscopy at 6 hrs.
Abbreviations: DOX, doxorubicin; Ab, antibody; NP, nanoparticle.

treated with DOX-NP/free-DOX, for 24 hrs indicates better efficacy of DOX-Ab-NP (Figure 6).

Cell cycle distribution analysis

Higher level of cell-arrest in S-phase by DOX-Ab-NP (for SKBR-3 cells 38.5% and for MCF-7 cells 28.3%) than by free-DOX (for SKBR-3 cells 22% and MCF-7 cells 8%)/ DOX-NP (for SKBR-3 cells 25% and for MCF-7 25.7%) demonstrates the potential of DOX-Ab-NP to distinctively inhibiting cellular proliferation in both the cell types (Figure 6).[41]

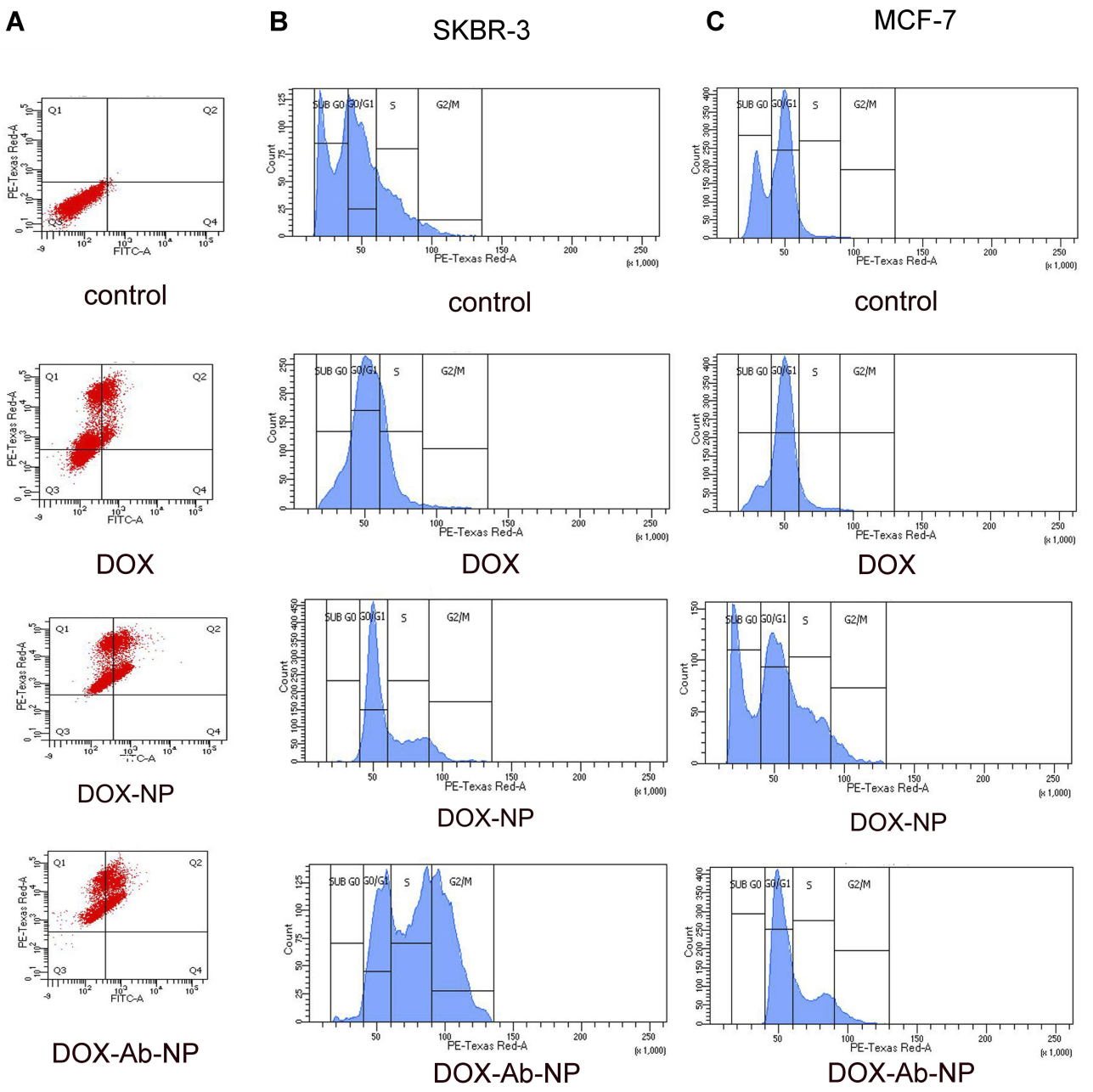

Figure 6 Apoptosis and cell cycle analysis data of breast cancer cells treated with experimental formulations and free-drug.
Notes: (**A**) Apoptosis study by flow cytometry of SKBR-3 cells with the treatment of free DOX, DOX –NP, and DOX-Ab-NP after 24 hrs. Cell cycle analysis by flow cytometry for (**B**) SKBR-3 cells and (**C**) MCF-7 cells treated with DOX, DOX-NP, and DOX-Ab-NP for 24 hrs.
Abbreviations: DOX, doxorubicin; Ab, antibody; NP, nanoparticle.

Caspase activation

HER2 expression

SKBR-3 has found to express the highest level of HER2 protein among all the three types of cells (Figure 7A). MDA-MB-231 cells expressed hardly any HER2.

Caspase activity

Caspase activity was maximum in SKBR-3/MCF-7 cells (Figure 7B) upon DOX-Ab-NP treatment compared to free-DOX/DOX-NP treatment. In MDA-MB-231 cells, a similar trend of caspase activity was found upon DOX-NP/DOX-Ab-NP administration.

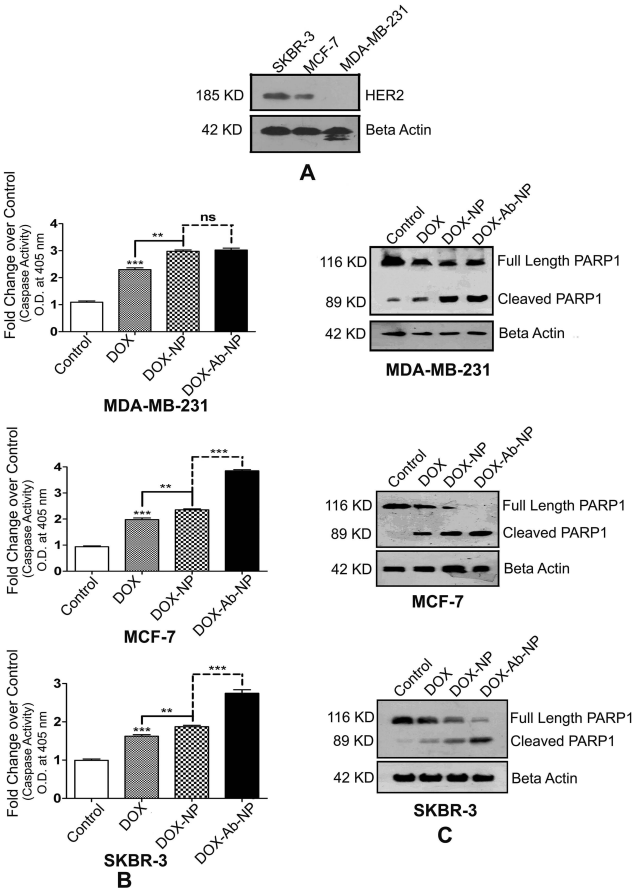

Figure 7 Comparative HER2 levels, caspase activity, and PARP cleavages in SKBR-3 cells, MCF-7 cells, and MDA-MB-231 cells.
Notes: (**A**) Determination of the relative level of HER2 in SKBR-3 cells, MCF-7 cells, and MDA-MB-231 cells. (**B**) Activation of Caspase in MDA-MB-231 cells, MCF-7 cells, and SKBR-3 cells. (**C**) Detection of PARP cleavage in MDA-MB-231 cells, MCF-7 cells, and SKBR-3 cells. The values of p show statistical level of significance, $^{**}p<0.05$, $^{***}p<0.01$, comparison between the groups are shown by over-head lines.
Abbreviations: DOX, doxorubicin; Ab, antibody; NP, nanoparticle.

Determination of apoptosis level

Western blots of PARP and cleaved product of PARP (Figure 7C) on SKBR-3 cells have shown that the blot intensity of PARP was more upon DOX-Ab-NP treatment than free-DOX treatment, suggesting for a higher level of apoptosis in SKBR-3 cells. A similar trend was seen in MCF-7 cells with a lower level of cleaved PARP1. DOX-NP/DOX-Ab-NP treated MDA-MB-231 cells indicated a similar level of PARP cleavage as the intensity of both the bands was similar.

In vivo studies

Pharmacokinetic study

The initial plasma DOX level was predominantly more upon free-DOX treatment than with the other formulations (Figure 8). But the drug eliminated faster from the body as shown by a higher clearance rate (Table 4).

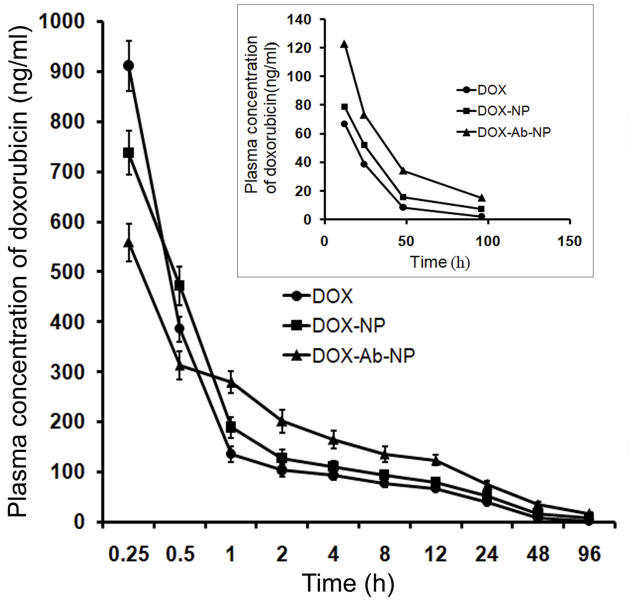

Figure 8 Plasma drug concentration upon IV bolus injection (at a dose of 10 mg/kg body weight) of DOX, DOX-NP, and DOX-Ab-NP. The same curve (time point 12–96 hrs) has been shown in the magnified version in the inset. Data show mean± SD (n=3).
Abbreviations: DOX, doxorubicin; Ab, antibody; NP, nanoparticle.

DOX-NP/DOX-Ab-NP retained longer in blood at least till 96 hrs (study duration) and released DOX in a sustained manner. The plasma half-life of DOX increased and clearance rate remarkably decreased upon DOX-NP/DOX-Ab-NP treatment than free-DOX treatment. The data were further supported by MRT values (Table 4).

In vivo cardiac toxicity study

Serum CK-MB and LDH levels were higher in free-DOX/DOX-NP/DOX-Ab-NP treated mice than the untreated control mice (Table 5). However, the values were in the order of DOX>DOX-NP>DOX-Ab-NP. SOD level in heart homogenate was found to decrease in free-DOX-treated mice compared to DOX-NP/DOX-Ab-NP treatment. Reduction of heart weights (heart excised 2 weeks after final dosing) upon free-DOX treatment than the other treatments (BL-NP/DOX-NP/DOX-Ab-NP) suggested that a marked reduction of cardiotoxicity occurred in mice upon DOX-Ab-NP treatment compared to free-DOX.

In the electrocardiography study, free-DOX treated mice showed a significant decrease of LV fractional shortening than all other groups of mice (Figure 9A). Minimum changes were observed in the case of DOX-NP, DOX-Ab-NP, and BL-NP treated group of animals. In histopathology, heart sections of the control group of mice showed normal-striated cells with centrally located nuclei whereas in BL-NP treated mice; there were no detectable histological changes and cardiotoxicity for

Table 4 Plasma pharmacokinetic parameters of free doxorubicin and doxorubicin released from DOX-NP and DOX-Ab-NP after intravenous bolus administration of DOX, DOX-NP, and DOX-Ab-NP with an equivalent amount of drug in BALB/c mice

Parameters	Plasma values of drug		
	Upon DOX administration	Upon DOX-NP administration	Upon DOX-Ab-NP administration
$t_{1/2}$ (hrs)	17.86±2.1	27.02±2.5[a]	32.78±2.9[a]
T_{max} (hrs)	0.25±0.021	0.25±0.02	0.25±0.023
C_{max} (ng/mL)	910.9±50.5	737.1±44.3[a]	558.5±37.9[a,b]
[§]AUC_{last} (hrs.ng/mL)	2880.1±199.2	3702.2±349.3	5663.5±440.2[a,b]
AUCinf (hrs.ng/mL)	2934.2±205.32	3986.8±333.33[a]	6382.5±448.4[a,b]
$AUMC_{last}$ (hrs.hrs.ng/mL)	46,707.8±2202.6	81,206.6±7111.5[a]	150,243.2±8200.1[a,b]
$AUMC_{inf}$ (hrs.hrs.ng/mL)	53,296.5±2600	119,611.4±1000.2[a]	253,262.5±1665.5[a,b]
MRT_{last} (hrs)	16.2±0.99	21.9±1.5[a]	26.5±2.02[a,b]
MRT_{inf} (hrs)	18.2±0.86	30.0±2.1[a]	39.7±2.33[a,b]
V_{ss} (L/Kg)	61.9±4.8	75.2±4.99[a]	62.2±5.2 [b]
C_L (L/hrs/kg)	3.4±0.24	2.5±0.19[a]	1.6±0.11 [a,b]

Notes: Significant difference corresponding from (I) DOX treatment [a]$p<0.05$, (ii) DOX-NP treatment [b]$p<0.05$. ‡Data show mean ± SD (n=3). [§]Units of AUC in plasma are hrs ng/mL, and in hepatic tissue hrs ng/g, respectively.

Abbreviations: DOX, doxorubicin; NP, nanoparticle; Ab, antibody; DOX, Free-drug, doxorubicin; DOX-NP, doxorubicin-loaded nanoparticles; DOX-Ab-NP, antibody conjugated doxorubicin loaded nanoparticles; $t_{1/2,}$ half-life; AUC_{last}, area under the plasma concentration–time curve from time 0 to time of last measurable concentration; AUC_{inf}, under the plasma concentration–time curve from time 0 infinity; $AUMC_{last}$, area under the first moment curve from time 0 to time of last measurable concentration; $AUMC_{inf}$, area under the first moment curve from time 0 to infinity; MRT, mean resident time; V_{ss}, steady state volume of distribution; CL, clearance.

Table 5 Doxorubicin-induced cardiotoxicity parameters of different formulations after 2 weeks of final dosing

Treatment group	Serum CK-MB (U/L)*	LDH (IU/L)*	% SOD*	Heart weight (g)*
Control (without any drug treatment)	44.44±3.1	142.32±8.12	100±7.3	0.1722±0.03
BL-NP	55.54±4.4	149.0±8.5	98.65±7.0	0.1662±0.022
Free-DOX	126.65±7.0[a,b]	250.10±11.7[a,b]	34.02±4.5[a,b]	0.1420±0.025
DOX-NP	70.20±5.6[a,b,c]	180.39±9.23[a,b,c]	42.78±5.1[a,b]	0.1650±0.019
DOX-Ab-NP	66.63±6.1[a,b,c]	166.67±8.8[c]	49.22±5.5[a,b]	0. 1670±0.036

Notes: *Data show mean ± SD (n=3). Significant difference corresponding from control [a]$p<0.05$, BL-NP; [b]$p<0.05$, Free-DOX; [c]$p<0.05$.

Abbreviations: CK-MB, creatine phosphokinase; LDH, lactate dehydrogenase; SOD, superoxide dismutase; BL-NP, blank nanoparticles; DOX, doxorubicin; DOX-NP, doxorubicin-loaded nanoparticles; DOX-Ab-NP, doxorubicin loaded antibody-conjugated nanoparticles.

the nanocarrier. Remarkable changes in degradation in cardiac muscle with vacuolization and edema of the cells were seen in the histopathology of heart sections of free-DOX-treated animals. Mild damage in heart muscle fibers in DOX-NP treated groups was observed. DOX-Ab-NP showed the comparatively better arrangement of the muscle with minimum damage (Figure 9B) possibly due to its higher tumor-specific delivery of drug and less availability for the cardiac tissue.[33,35]

In vivo imaging by radiolabeled nanoparticles

Gamma scintigraphy and biodistribution

After 4 hrs of administration of radiolabeled free-DOX/DOX-NP/DOX-Ab-NP, gamma scintigraphic images showed their accumulation in the order of ^{99m}Tc DOX-Ab-NP>^{99m}Tc DOX-NP>^{99m}Tc DOX in the xenograft tumor area (Figure 10A(d–f)). The very poor signal was found for ^{99m}Tc-DOX in the tumor region (Figure 10A(d)). Images (Figure 10A) also showed poorer cardiac accumulation of ^{99m}Tc-DOX-Ab-NP.

The biodistribution study through IV injected ^{99m}Tc-DOX/^{99m}Tc-DOX-NP/^{99m}Tc-DOX-Ab-NP showed that a predominant accumulation of ^{99m}Tc-DOX-Ab-NP took place in the tumor region compared to ^{99m}Tc-DOX-NP/^{99m}Tc-DOX treatment. Accumulations of ^{99m}Tc-DOX/^{99m}Tc-DOX-NP/^{99m}Tc-DOX-Ab-NP were observed in liver, kidney, intestine, and urinary bladder (Table 6).

In vivo therapeutic study on tumor-bearing xenograft mice

Tumor volumes were reduced upon the treatment of DOX/DOX-NP/DOX-Ab-NP in mice in the order of DOX-Ab-NP>DOX-NP>DOX (Figure 10B(a)). The mice received normal saline did not show any effect on tumor reduction.

Mice treated with DOX-Ab-NP showed an average tumor volume of 253.33 mm^3 on day 15 and 823 mm^3 on day 25 (Figure 10B(a)). For DOX-NP treated group, the value was 350 mm^3 on day 15 and 1343.33 mm^3 on day 25. The DOX-

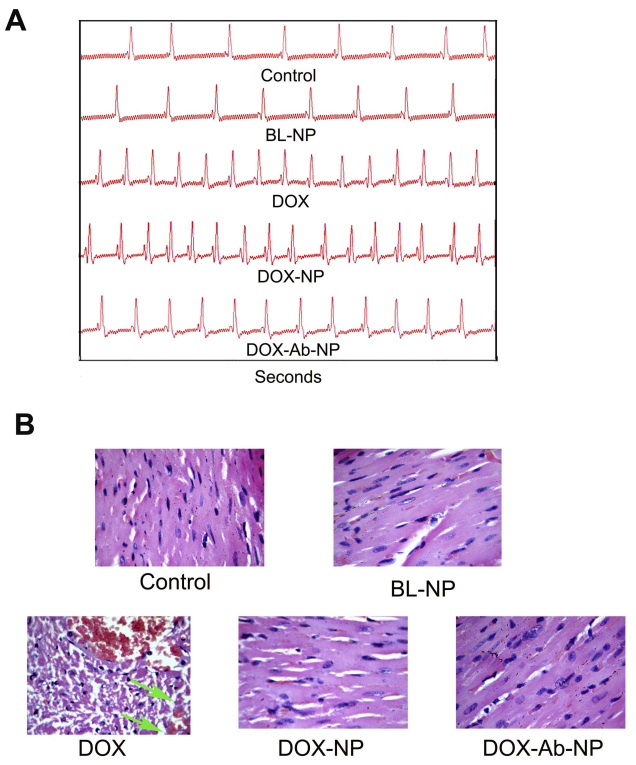

Figure 9 Comparative cardiotoxicity profiles by the treatment of DOX, BL-NP, DOX-NP, and DOX-Ab-NP.
Notes: (**A**) Echocardiography images. (**B**) Histopathology of cardiac tissue (Vascularization due to free-drug treatment was shown by the green arrow in the respective image).
Abbreviations: DOX, doxorubicin; Ab, antibody; NP, nanoparticle.

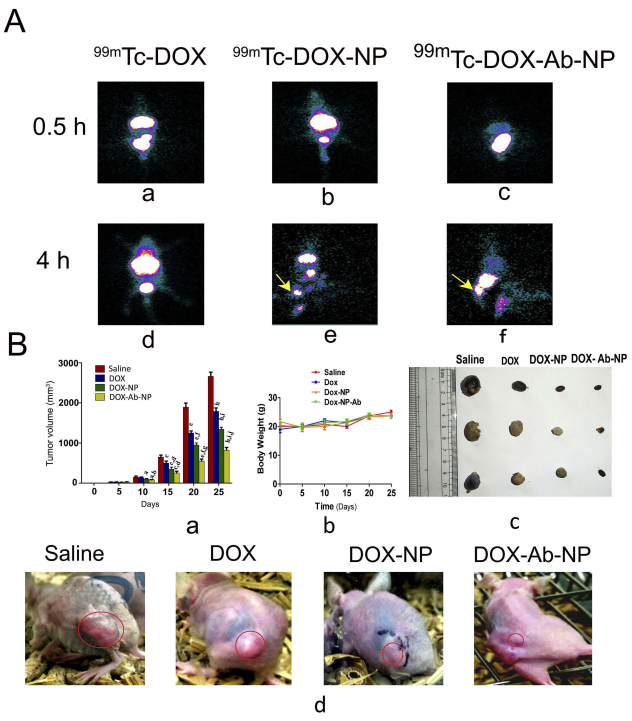

Figure 10 Biodistribution of drug/formulation data and, tumor and tumor-related data in experimental animals.
Notes: (**A**) Biodistribution and accumulation data of ^{99m}Tc labeled drug/formulations in experimental mice (a) time-dependent biodistribution and accumulation of ^{99m}Tc-DOX at 0.5 hrs (d) and at 4 hrs, (b) ^{99m}Tc -DOX-NP at 0.5 hrs (e) and 4 hrs, and (**c**) ^{99m}Tc -DOX-Ab-NP at 0.5 hrs and (f) 4 hrs, in xenograft mice-bearing breast tumor. (**B**) Changes in tumor volume, animal body weight, and excised tumors from the experimental mice along with the tumor growth-related representative visual image data. (a) Relative changes in tumor volume with time. Data showed mean tumor volume (mean ± SD, n=3) in different experimental and control mice. The value $p<0.05$ shows the level of statistical significance. Prefix of p (i.e., a–j), indicates as mentioned below: "a" indicates statistical level of significance when data were compared against normal saline treated (control) mice on day 10; "b" indicates statistical level of significance when data were compared against DOX-treated mice on day 10; "c" indicates statistical level of significance when data were compared against normal saline treated (control) mice on day 15; "d" indicates statistical level of significance when data were compared against DOX-treated mice on day 15; "e" indicates statistical level of significance when data were compared against normal saline treated (control) mice on day 20; "f" indicates statistical level of significance when data were compared against DOX-treated mice on day 20; "g" indicates statistical level of significance when data were compared against DOX-NP-treated mice on day 20; "h" indicates statistical level of significance when data were compared against normal saline treated (control) mice on day 25; "i" indicates statistical level of significance when data were compared against DOX-treated mice on day 25; "j" indicates statistical level of significance when data were compared against DOX-NP-treated mice on day 25. (b) Change of body weight of nude mice-bearing tumor. Data represent mean ± SD (n=3); data showed that there was no statistically significant variation between the groups of mice. (c) Tumors excised from the experimental mice after treatment with saline/DOX/DOX-NP/DOX-Ab-NP. (d) Images on day 25 of nude mice bearing SKBR-3 tumor after treatment with saline/DOX/DOX-NP/DOX-Ab-NP. Tumor areas have been marked with red circles in the figure.
Abbreviations: ^{99m}Tc-DOX: radiolabeled free-doxorubicin, ^{99m}Tc-DOX -NP: radiolabeled doxorubicin loaded nanoparticles, ^{99m}Tc-DOX-Ab-NP: radiolabeled doxorubicin loaded antibody conjugated nanoparticles; DOX, doxorubicin; Ab, antibody; NP, nanoparticle.

treated group had a tumor volume 500 mm^3 on day 15 and 1790 mm^3 on day 25 and saline-treated control mice had an average tumor volume of 650 mm^3 on day 15 and 2663 mm^3 on day 25. Data suggest that DOX-Ab-NP showed maximum tumor suppression effect among the tested formulations and free-DOX. Nanocarriers were found to be more efficacious than free-drug. The change in body weight of all the treated mice was insignificant (Figure 10B(b)). Individual tumor volume curves (Figure S4) and tumor weights at the terminal experiment showed DOX-Ab-NP was most efficient among the experimental treatments to control tumor progression in the experimental animals. The data showed that the trend of tumor progression was similar at pace in the experimental mice. Average tumor weights of the excised tumors from normal saline/free DOX/DOX-NP/DOX-Ab-NP treated group of animals were 1.003±0.16 g, 0.424±0.06 g, 0.111 ±0.016 g, 0.061±0.009 g, respectively. Images for individual tumors excised from respective groups of animals have been shown in Figure 10B(c). Representative image of tumors on the experimental mice has been shown in Figure 10B(d).

Discussion

This study offers the technology how to incorporate a highly water-soluble drug into a hydrophobic polymeric

Table 6 Biodistribution data of ^{99m}Tc-DOX, ^{99m}Tc-DOX-NP, ^{99m}Tc-DOX-Ab-NP in mice after IV. administration

Organ/Tissue	^{99m}Tc-DOX	^{99m}Tc-DOX-NP	^{99m}Tc-DOX-Ab-NP
Blood	0.118±0.04	0.223±0.031[a]	0.526±0.05[a,b]
Heart	0.125±0.035	0.065±0.008[a]	0.006±0.001[a,b]
Liver	5.854±0.13	17.67±2.7[a]	18.231±3[a]
Lung	0.153±0.044	2.561±0.18[a]	2.926±0.19[a]
Spleen	0.052±0.01	0.122±0.06	0.351±0.052[a,b]
Muscle	0.042±0.012	0.039±0.01	0.028±0.009
Kidney	5.380±0.18	2.181±0.11[a]	2.921±0.21[a,b]
Intestine	2.990±0.14	4.245±0.19[a]	5.105±0.25[a,b]
Stomach	0.167±0.05	0.223±0.03	0.251±0.04
Urine	21.25±3.6	12.214±2.6[a]	11.91±2.1[a]
Tumor	0.100±0.045	0.167±0.06	0.356±0.044[a,b]

Notes: *Data show mean ± SD (n=3). Significant difference corresponding from DOX [a]$p<0.05$, DOX-NP; [b]$p<0.05$.
Abbreviations: DOX, doxorubicin; Ab, antibody; NP, nanoparticle; ^{99m}Tc-DOX, radiolabeled free-doxorubicin; ^{99m}Tc-DOX –NP, radiolabeled doxorubicin-loaded nanoparticles; ^{99m}Tc-DOX-Ab-NP, radiolabeled doxorubicin-loaded antibody-conjugated nanoparticles.

nanocarrier by restricting drug leaching upon optimizing pH of the aqueous phase of the emulsion and thus, improvement of drug entrapment during the development of the formulation and to provide a long-term sustained drug release. Alkaline pH (pH 8) of the aqueous media resulted in a drastic increase in drug loading which may be due to the reduced solubility of DOX at alkaline pH and simultaneous precipitation of drug and polymer.[42] Tween 80 resulted in spherical particles along with the maximum drug. Therefore, nanoparticles developed with tween 80 were optimized further for ligand conjugation. In-situ incorporation of the spacer molecule, BS3 (contains an amine-reactive N-hydroxy sulphosuccinimide (NHS) ester at each end of an 8-carbon spacer arm), without altering the formulation conditions produced activated DOX-containing NP for further antibody attachment. This non-covalent insertion of linker molecules provides advantages over other nanoparticle surface functionalization techniques.[18] The terminal hydrophilic sulphonyl groups of BS3 arranged themselves in such a pattern on the outer surface of PLGA nanoparticles that they facilitated the reaction between NHS ester with primary amines of the antibody (at pH 7–9) providing a stable amide bond by releasing NHS group.[22]

HER2 protein provides a convincing target for immunotherapy due to its overexpression (20–30% of the breast cancer types), surface accessibility and preferred accumulation of antibody-conjugated nanocarriers through receptor-mediated endocytosis.[43] Trastuzumab is only United States-Food and Drug Administration (US-FDA) approved humanized antibody used for immunotherapy in the treatment of advanced breast cancer.[44] Although combined therapy with anthracycline has been reported to cause elevated cardiotoxicity, conjugation of anti-HER2(CD-340)-antibody in sub-therapeutic concentration facilitates the treatment of drug-loaded nanocarriers specifically to target cells. Thus, it may reduce cardiotoxicity. In this study, HER2 (CD-340)-antibody was successfully conjugated at its concentration below therapeutic dose (that acts as a targeting ligand rather than a therapeutic agent).[44]

FTIR data confirmed the absence of any chemical interaction between DOX and the excipients, but the minor shifting of peaks was observed due to some physical interactions. Further, a comparative analysis of the FTIR spectra showed the noncovalent insertion of BS3 on the surface of DOX-NP. EDX study reveals that the presence of nitrogen in DOX-NP and absence of it in BL-NP which suggests the presence/absence of nitrogen of DOX in the two respective formulations. EDX data of BL-NP-BS and DOX-BS-NP showed that sulfur was present in both of the formulations but is not in BL-NP or DOX-NP. Data have confirmed the presence of BS3 in BL-NP-BS and DOX-BS-NP.

Physical characterization showed that the antibody unconjugated and conjugated particles were oval to spherical and within the size range of 200–250 nm. Particle size slightly increased for antibody-conjugated nanoparticles (DOX-Ab-NP). Again, SEM images showed an uneven surface for DOX-Ab-NP which had a smooth surface before conjugation. AFM images further confirmed the uneven surface of DOX-Ab-NP. TEM images showed a dense distribution of drug particles inside the polymer matrix. An increase zeta potential of DOX-Ab-NP was possibly due to the incorporation of antibody.[23] Zeta potential data and stability study

data suggest that the lyophilized nanoparticles were stable at 4–8°C and require to suspend in water for injection before its intravenous administration.

Faster release of DOX in citrate buffer (pH 3) than in PBS with tween 80, and HBC might be due to a faster dissociation of polylactic acid-glycolic acid polymer (Figure 2). In acidic conditions (pH 3), the media catalyzed the hydrolysis of PLGA core by attacking ester bonds causing a faster degradation of the polymer. But on alkaline pH (pH 10), the polymer tended to keep its non-polar character by entrapment of hydroxyl group on polymer surface and lowered the water absorption by particles which in turn led to a more stable condition of nanoparticles in higher pH media. In neutral or slightly acidic pH (pH 7.4 and 5), the hydrolytic degradation was low to moderate. The faster drug release pattern in acidic condition (pH 5) than in PBS (pH 7.4) particularly demonstrates the faster release of DOX from DOX-Ab-NP in acidic tumor environment than in the physiologically neutral media of blood during circulation. This could facilitate better drug release in the tumor environment.[36] A good linearity in the kinetics (determined by R^2 value) in tween 80 buffer, citrate buffer, and in acetate buffer suggests release of DOX followed Korsmeyer–Peppas kinetic that shows an anomalous drug diffusion pattern, whereas, in PBS buffer, bicarbonate buffer, and HPBCD media, drug release followed Higuchi kinetics suggesting for drug diffusion from matrix system.

Particle morphology of HER2 (CD-340) unconjugated and conjugated particles revealed that PLGA polymeric matrix could not withstand higher temperature (40°C) at 85% RH, causing softening of PLGA. Particles remained moderately stable for 3 months at 30°C with 55% RH and fully stable at 4°C (refrigerated condition).

TEM images of antibody-conjugated nanoparticles showed the presence of a brighter part surrounding the core which was absent for antibody-unconjugated nanoparticles. This might be due to the presence of FITC-conjugated antibody on the surface. FACS analysis showed a 10% increment in the FITC region for antibody-conjugated DOX-Ab-NP compared to unconjugated DOX-NP. To reconfirm the antibody attachment, we performed the confocal microscopy. The larger size BL-NP were prepared by reducing the homogenization speed and sonication time for visualization of the particles by confocal microscopy. The FITC-tagged antibody was clearly shown to be present on the nanoparticle surface in the confocal images of antibody-conjugated BL-NP and thus confirms the attachment of the anti-HER2 (CD-340) antibody to the DOX-NP surface. Gel electrophoresis further confirmed the attachment of antibodies.

DOX-Ab-NP/DOX-NPs were internalized by endocytosis which might follow endosomal escape and delivered the encapsulated drug to the cytosol.[45] Higher intracellular delivery of the nanoparticles usually reflects the efficacy of encapsulated DOX.[46] Hence, less dose could be capable of producing a higher cytotoxic effect than free-drug. DOX-Ab-NP cytotoxicity toward SKBR-3 cells (overexpressing HER2), MCF-7 (expresses HER2 weakly)[47] and MDA-MB-231 (Triple-negative cells) showed that DOX-Ab-NP had higher cytotoxicity than DOX-NP in the cells. DOX-Ab-NP/DOX-NP might slowly release drug over a longer period causing sustained toxicity[23] which could increase apoptosis and enhance cell cycle arrest in highly HER2-overexpressed SKBR-3 cells. Higher cellular toxicity was further correlated with the higher cellular uptake of DOX-Ab-NP.

DOX acts by inhibiting the topoisomerase activity which disrupts the regulation of cell cycle in S-phase and cells are unable to cross the S-G2 transition in cancer cells.[48] An excessive DNA damage in S-phase might be one of the major causes of cell death, showing considerable cell arrest at S-phase for DOX-NP/DOX-Ab-NP treatment than that of free-DOX. Since MCF-7 cells have lower expression of HER2, DOX-NP-Ab treatment did not show a pronounced S-phase cell arrest on MCF-7 cells as seen in SKBR-3 cells.

SKBR-3 cells had expressed the highest level of HER2 protein followed by MCF-7. MDA-MB-231 cells were devoid of HER2 expression. The cleavage of PARP1 is done by caspase, preventing DNA repairing which ultimately leads to apoptosis.[49] Caspase levels were maximum upon DOX-Ab-NP treatment in SKBR-3 and MCF-7 cells. However, MDA-MB-231 cells had similar levels of caspase upon DOX-Ab-NP and DOX-NP treatments. The conjugation of the antibody to the nanoparticle surface increased cellular targeting and internalization capabilities of the nanocarrier in HER2 expressed breast cancer cells, causing an increased level of apoptosis in the neoplastic cells.[50]

A significant recovery of the cardiotoxicity marker levels was observed (Table 5) in DOX-Ab-NP/DOX-NP treated animals than the free-DOX treatment. Heart tissue structure was well preserved upon DOX-Ab-NP/DOX-NP treatment whereas tissue damage was observed in free-DOX-treated animals. Findings were also supported by

the echocardiogram. Thus, DOX-Ab-NP significantly reduced cardiotoxicity of DOX by making it less and slowly available with a quicker clearance for the heart muscles.

The enhanced biological half-life of DOX was observed upon DOX-NP/DOX-Ab-NP treatment compared to free-DOX treatment. C_{max} values were comparatively less for DOX-NP and DOX-Ab-NP but AUC and AUMC values were significantly higher, which showed better anticancer efficacy of those formulations than free-DOX. Higher MRT also indicates prolonged and systemic availability of DOX. Comparatively, less clearance value of DOX-NP/DOX-Ab-NP further supported the findings.

Semete et al 2010, showed by experimental data that a large amount of PLGA nanoparticle was present in kidney and liver, without causing any morphological changes in respective tissues, even at high dose of PLGA which emphasizes the fact that PLGA nanoparticles are safe in kidney and liver when they are used to deliver any incorporated drug.[51] The US-FDA has also recommended it as nontoxic and safe for human use. There is no report of its toxic effect on kidney and liver.[52]

The distinct tumor-targeting capacity of ^{99m}Tc-DOX-Ab-NP was seen in gamma scintigraphy images, compared to ^{99m}Tc-DOX-NP. The less extent of accumulation of ^{99m}Tc-DOX-Ab-NP in heart also explains the reason for the nanoformulations to show less cardiotoxicity. The higher amount of accumulation in the tumor suggests that DOX-Ab-NP successfully targeted the tumor.[35]

Enhanced therapeutic potency with no significant change in the body weight in SKBR3 tumor-bearing mice treated with DOX-Ab-NP supports the site-specific drug delivery ability of the formulation and therapeutic potential of formulated nanocarriers in the treatment of HER2-overexpressed breast cancers.

Conclusion

In this study, antibody-conjugated DOX-loaded PLGA nanoparticles showed a promise in improving the tumor site-specific delivery of the drug with a significant reduction of drug-related cardiac toxicity. DOX-NP showed therapeutic improvement over free-DOX but not up to the extent of DOX-Ab-NP. Hence, DOX-Ab-NP could be a preferential choice to more specifically deliver the drug in HER2-overexpressed breast cancer cells, with an additional safety of heart.

The present formulation has the potential to preferentially deliver drug to the neoplastic cells, causing reduction of DOX-mediated cardiotoxicity due to its more site-specific distribution of drug to the target site. Further, due to sustained drug release from the formulation much less free-drug was available for heart and other parts of body tissue to cause toxicity. Thus, this formulation may be future hope to deliver drug to the target tissue and also minimize cardiotoxicity of the drug. However, the major limitation of this antibody-conjugated formulation is the saturation of cell surface target protein (antigen). Once the surface antigen proteins are saturated, the formulation would not be able to target the neoplastic cells only and prolong presence without its distribution in neoplastic cells may affect normal cells also. Thus, the dose should be optimized before administration of formulation.

Hence, further studies including clinical trials are warranted to optimize the dose in human subjects and to investigate the potential of the formulation in the human breast cancer patients.

Ethical conduct of research

The experimental protocol of the study was approved by the Institutional Animal Ethics Committee of Jadavpur University, Kolkata. Animal care was in accordance with the Committee for the Purpose of Control and Supervision of Experiments on Animals guidelines.

Acknowledgment

Authors are indebted to the Indian Council of Medical Research for providing the financial grant (Ref No 45/6/2013Nan/BMS dated 24.02.2015) and Doctoral Scholarship under RUSA 2.0 Scheme (Ref No R-11/144/19 dated 25/02/2019) to conduct the study.

The authors acknowledge Dr. Sanmoy Karmakar and Rudranil Bhowmik for helping in technical issues related to the Echocardiography study in mice.

Disclosure

The authors of this article have no conflict of interest to declare with regard to this work.

References

1. Siegel RL, Miller KD, Jemal A. Cancer statistics, 2016. *CA Cancer J Clin*. 2016;66:7–30. doi:10.3322/caac.21332
2. Mirakabad FST, Nejati-Koshki K, Akbarzadeh A, et al. PLGA-based nanoparticles as cancer drug delivery systems. *Asian Pac J Cancer Prev*. 2014;15(2):517–535. doi:10.7314/apjcp.2014.15.2.517
3. Mukherjee B, Das S, Chakraborty S, et al. Potentials of polymeric nanoparticle as drug carrier for cancer therapy: with a special reference to pharmacokinetic parameters. *Curr Drug Metab*. 2015;15(6):565–580. doi:10.2174/1389200215666140605150703

4. Alatrash G, Molldrem JJ. Tumor-associated antigens. In: Socié G, Blazar BR editors. *Immune Biology of Allogeneic Hematopoietic Stem Cell Transplantation.Models in Discovery and Translation*. Academic Press. ISBN: 978-0-12-416004-0; 2013 143–164.
5. Mukherjee B. Nanosize drug delivery system. *Curr Pharm Biotechnol*. 2013;14(15):1221.
6. Xi J, Li M, Jing B, et al. Long-circulating amphiphilic doxorubicin for tumor mitochondria specific targeting. *ACS Appl Mater Interfaces*. 2018;10:43482−43492. doi:10.1021/acsami.8b17399
7. Lv S, Li M, Tang Z, et al. Doxorubicin-loaded amphiphilic polypeptide-based nanoparticles as an efficient drug delivery system for cancer therapy. *Acta Biomater*. 2013;9(12):9330–9342. doi:10.1016/j.actbio.2013.08.015
8. Gabizon A, Shmeeda H, Barenholz Y. Pharmacokinetics of pegylated liposomal doxorubicin. *Clin Pharmacokinet*. 2003;42(5):419–436. doi:10.2165/00003088-200342050-00002
9. Criscitiell C. Tumor-associated antigens in breast cancer. *Breast Care*. 2012;7:262–266. doi:10.1159/000342164
10. Wold ED, Smider VV, Felding BH. Antibody therapeutics in oncology. *Immunotherapy*. 2016;2(1):1–18. doi:10.4172/2471-9552.1000108
11. Mukherjee B, Satapathy BS, Mondal L, Dey NS, Maji R. Potentials and challenges of active targeting at the tumor cells by engineered polymeric nanoparticles. *Curr Pharm Biotechnol*. 2013;14(15):1250–1263.
12. Yoo J, Park C, Yi G, Lee D, Koo H. Active targeting strategies using biological ligands for nanoparticle drug delivery systems. *Cancers*. 2019;11:640. doi:10.3390/cancers11050640
13. Fahmy TM, Fong PM, Goyal A, Saltzman WM. Targeted for drug delivery. *Nanotoday*. 2005;8(8):18–26.
14. Iqbal N, Iqbal N. Human epidermal growth factor receptor 2 (HER2) in cancers: overexpression and therapeutic implications. *Hindawi Publishing Corporation*. 2014;2014:9. Article ID 852748.
15. Breastcancer. Pennsylvania: HER2 status. 2019. Available from: https://www.breastcancer.org/symptoms/diagnosis/her2 Accessed August 12, 2019.
16. Biolegend. United States: FITC anti-human CD340 (erbB2/HER-2) Antibody. 2019. Available from https://www.biolegend.com/en-us/products/fitc-anti-human-cd340-erbb2-her-2-antibody-3765. Accessed August 14, 2019.
17. Maji R, Dey NS, Satapathy BS, Mukherjee B, Mondal S. Preparation and characterization of tamoxifen citrate loaded nanoparticles for breast cancer therapy. *Int J Nanomedicine*. 2014;9:3107–3118. doi:10.2147/IJN.S63535
18. Thamake SI, Raut SL, Ranjan AP, Gryczynski Z, Vishwanatha JK. Surface functionalization of PLGAnanoparticles by non-covalent insertion of a homo-bifunctional spacer for active targeting in cancer therapy. *Nanotechnology*. 2011;22(3):035101–0351011. doi:10.1088/0957-4484/22/3/035101
19. Das PJ, Paul P, Mukherjee B, et al. Pulmonary delivery of voriconazole loaded nanoparticles providing a prolonged drug level in lungs: a promise for treating fungal infection. *Mol Pharm*. 2015;12(8):2651–2664. doi:10.1021/acs.molpharmaceut.5b00064
20. Dutta L, Mukherjee B, Chakraborty T, et al. Lipid-based nanocarrier efficiently delivers highly water soluble drug across the blood-brain barrier into brain. *Drug Deliv*. 2018;25(1):504–516. doi:10.1080/10717544.2018.1474967
21. Bhattacharya S, Mondal L, Mukherjee B, Dutta L, Ehsan I, Debnath MC. Apigenin loaded nanoparticle delayed development of hepatocellular carcinoma in rats. *Nanomedicine*. 2018;14(6):1905–1917. doi:10.1016/j.nano.2018.05.011
22. Mukerjee A, Ranjan AP, Vishwanatha JK, Helson L. Non-covalent surface integration: optimizing a novel technique for preparing targeted polymeric nanoparticles for cancer therapeutics. *Int J Nanotechnol*. 2014;11(5/6/7/8):676–685. doi:10.1504/IJNT.2014.060590
23. Chen H, Gao J, Lu Y, et al. Preparation and characterization of PE38KDEL-loaded anti-HER2 nanoparticles for targeted cancer therapy. *J Control Release*. 2008;128(3):209–216. doi:10.1016/j.jconrel.2008.03.010
24. Kocbek P, Obermajer N, Cegnar M, Kos J, Kristl J. Targeting cancer cells using PLGA nanoparticles surface modified with a monoclonal antibody. *J Control Release*. 2007;120(1–2):18–26. doi:10.1016/j.jconrel.2007.03.012
25. Das K, Prasad R, Singh A, et al. Protease-activated receptor 2 promotes actomyosin dependent transforming microvesicles generation from human breast cancer. *Mol Carcinog*. 2018;57(12):1707–1722. doi:10.1002/mc.22891
26. Mandal D, Shaw TK, Dey G, et al. Preferential hepatic uptake of paclitaxel-loaded poly-(D-L-lactide-co-glycolide) nanoparticles- A possibility for hepatic drug targeting: pharmacokinetics and biodistribution. *Int J Biol Macromol*. 2018;112:818–830. doi:10.1016/j.ijbiomac.2018.02.021
27. Sahoo SK, Labhasetwar V. Enhanced antiproliferative activity of transferrin-conjugated paclitaxel-loaded nanoparticles is mediated via sustained intracellular drug retention. *Mol Pharm*. 2005;2(5):373–383. doi:10.1021/mp050032z
28. Zeng X, Morgenstern R, Nyström AM. Nanoparticle-directed sub-cellular localization of doxorubicin and the sensitization of breast cancer cells by circumventing GST-Mediated drug resistance. *Biomaterials*. 2014;35(4):1227–1239. doi:10.1016/j.biomaterials.2013.10.042
29. Parveen S, Sahoo SK. Evaluation of cytotoxicity and mechanism of apoptosis of doxorubicin using folate-decorated chitosan nanoparticles for targeted delivery to retinoblastoma. *Cancer Nano*. 2010;1(1–6):47–62. doi:10.1007/s12645-010-0006-0
30. Ding L, Tian C, Feng S, Fida G, Zhang C, Ma Y. Small sized EGFR1 and HER2 specific bifunctional antibody for targeted cancer therapy. *Theranostics*. 2015;5(4):378–398. doi:10.7150/thno.10084
31. Peterson QP, Goode DR, West DC, Botham RC, Hergenrother PJ. Preparation of the caspase-3/7 substrate Ac-DEVD-pNA by solution-phase peptide synthesis. *Nat Protoc*. 2010;5(2):294–302. doi:10.1038/nprot.2009.149
32. Ma W, Wang J, Guo Q, Tu P. Simultaneous determination of doxorubicin and curcumin in rat plasma by LC–MS/MS and its application to pharmacokinetic study. *J Pharm Biomed Anal*. 2015;111:215–221. doi:10.1016/j.jpba.2015.04.007
33. Park J, Fong PM, Lu J, et al. PEGylated PLGA nanoparticles for the improved delivery of doxorubicin. *Nanomedicine*. 2009;5(4):410–418. doi:10.1016/j.nano.2009.02.002
34. Myers CE, McGuire WP, Liss RH, Ifrim I, Grotzinger K, Young RC. Adriamycin: the role of lipid peroxidation in cardiac toxicity and tumor response. *Science*. 1977;197(4299):165–167. doi:10.1126/science.877547
35. Jain AK, Swarnakar NK, Das M, et al. Augmented anticancer efficacy of doxorubicin-loaded nanoparticles after oral administration in a breast cancer induced animal model. *Mol Pharm*. 2011;8(4):1140–1151. doi:10.1021/mp200011f
36. Choi WI, Lee JH, Kim JY, et al. Targeted antitumor efficacy and imaging via multifunctional nano-carrier conjugated with anti-HER2 trastuzumab. *Nanomedicine*. 2015;11(2):359–368. doi:10.1016/j.nano.2014.09.009
37. Gaonkar RH, Ganguly S, Dewanjee S, et al. Garcinol loaded vitamin E TPGS emulsified PLGA nanoparticles: preparation, physicochemical characterization, in vitro and in vivo studies. *Sci Rep*. 2016;7(530):1–14.
38. Satapathy BS, Mukherjee B, Baishya R, Debnath MC, Dey NS, Maji R. Lipid nanocarrier based transport of docetaxel across the blood-brain barrier. *RSC Adv*. 2016;6(88):85261–85274. doi:10.1039/C6RA16426A
39. Chakraborty S, Ehsan I, Mukherjee B, et al. Therapeutic potential of andrographolide-loaded nanoparticles on a murine asthma model. *Nanomedicine*. 2019;20:102006. doi:10.1016/j.nano.2019.04.009

40. Chung YI, Kim JC, Kim YH, et al. The effect of surface functionalization of PLGA nanoparticles by heparin- or chitosan-conjugated Pluronic on tumor targeting. *J Control Release*. 2010;143(3):374–382. doi:10.1016/j.jconrel.2010.01.017 Epub 2010 Jan 25.
41. Jiang D, Lynch C, Medeiros CB, Liedtke M, Bam R, Tam AB. Identification of doxorubicin as an inhibitor of the ire1α-xbp1 axis of the unfolded protein response. *Sci Rep*. 2016;6:33353. doi:10.1038/srep33353
42. Khemani M, Sharon M, Sharon M. pH-Dependent Encapsulation of Doxorubicin in PLGA. *Ann Biol Res*. 2012;3(9):4414–4441.
43. Cirstoiu-Hapca A, Buchegger F, Bossy L, Kosinski M, Gurny R, Delie F. Nanomedicines for active targeting: physico-chemical characterization of paclitaxel-loaded anti-HER2 immuno nanoparticles and in vitro functional studies on target cells. *Eur J Pharm Sci*. 2009;38(3):230–237. doi:10.1016/j.ejps.2009.07.006
44. Yousefpour P, Atyabi F, Vasheghani-Farahani E, Movahedi AA, Dinarvand R. Targeted delivery of doxorubicin-utilizing chitosan nanoparticles surface-functionalized with anti-Her2 trastuzumab. *Int J Nanomedicine*. 2011;6:1977–1990. doi:10.2147/IJN.S25646
45. Kim S-W, Khang D. Multiple cues on the physiochemical, mesenchymal, and intracellular trafficking interactions with nanocarriers to maximize tumor target efficiency. *Int J Nanomedicine*. 2015;10:3989–4008.
46. Shen H, Ackerman AL, Cody V, Giodini A, Hinson ER, Cresswell P. Enhanced and prolonged cross-presentation following endosomal escape of exogenous antigens encapsulated in biodegradable nanoparticles. *Immunology*. 2006;117(1):78–88. doi:10.1111/j.1365-2567.2005.02268.x
47. Merlin JL, Barberi-Heyob M, Bachmann N. In vitro comparative evaluation of trastuzumab (Herceptin®) combined with paclitaxel (Taxol®) or docetaxel (Taxotere®) in HER2-expressing human breast cancer cell lines. *Ann Oncol*. 2002;13(11):1743–1748. doi:10.1093/annonc/mdf263
48. Siddharth S, Nayak A, Nayak D, Bindhani BK, Kundu CN. Chitosan-Dextran sulfate coated doxorubicin loaded PLGA-PVA nanoparticles caused apoptosis in doxorubicin resistance breast cancer cells through induction of DNA damage. *Sci Rep*. 2017;7:2143. doi:10.1038/s41598-017-02134-z
49. Los M, Mozoluk M, Ferrari D, Stepczynska A, Stroh C, Renz A. Activation and caspase-mediated inhibition of PARP: A molecular switch between fibroblast necrosis and apoptosis in death receptor signaling. *Mol Biol Cell*. 2002;13(3):978–988. doi:10.1091/mbc.01-05-0272
50. Chaitanya G, Steven AJ, Babu PP. PARP-1 cleavage fragments: signatures of cell-death proteases in neurodegeneration. *Cell Commun Signal*. 2010;8(31):1–11. doi:10.1186/1478-811X-8-1
51. Semete B, Booysen L, Lemmer Y, et al. In vivo evaluation of the biodistribution and safety of PLGA nanoparticles as drug delivery systems. *Nanomedicine*. 2010;6(5):662–671. doi:10.1016/j.nano.2010.02.002
52. Navarro SM, Morgan TW, Astete CE, et al. Biodistribution and toxicity of orally administered poly(lactic-co-glycolic) acid nanoparticles to F344 rats for 21 days. *Nanomedicine*. 2016;11(13):1653–1669. doi:10.2217/nnm-2016-0233